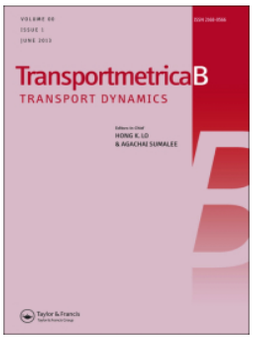

Transportmetrica B: Transport Dynamics

ISSN: (Print) (Online) Journal homepage: https://www.tandfonline.com/loi/ttrb20

A Kriging-based optimization method for meeting point locations to enhance flex-route transit services

Mingyang Li, Jinjun Tang, Jie Zeng & Helai Huang

To cite this article: Mingyang Li, Jinjun Tang, Jie Zeng & Helai Huang (2023) A Kriging-based optimization method for meeting point locations to enhance flex-route transit services, Transportmetrica B: Transport Dynamics, 11:1, 1281-1310, DOI: 10.1080/21680566.2023.2195984

To link to this article: https://doi.org/10.1080/21680566.2023.2195984

Published online: 03 Apr 2023.

TRANSPORTMETRICA B: TRANSPORT DYNAMICS
2023, VOL. 11, NO. 1, 1281–1310
https://doi.org/10.1080/21680566.2023.2195984

A Kriging-based optimization method for meeting point locations to enhance flex-route transit services

Mingyang Li, Jinjun Tang, Jie Zeng and Helai Huang

Smart Transportation Key Laboratory of Hunan Province, School of Traffic and Transportation Engineering, Central South University, Changsha, People's Republic of China

ABSTRACT

As a promising on-demand transportation mode in low-demand areas, flex-route transit, has attracted much attention in the transportation research field. However, unexpectedly high demand levels caused by travel uncertainty impact the reliability and development of flex-route transit services. Although the meeting point strategy can deal with this problem effectively, selecting a location for the meeting points can substantially influence the performance of this strategy. In this study, meeting point location selection is modeled as a simulation-based optimization (SO) problem, and a Kriging-based global optimization method using a Pareto-based multipoint sampling strategy (KGO-PS) is proposed to solve this problem. Through comparison of several typical benchmark functions with other counterparts, the effectiveness of KGO-PS has been verified. Moreover, a real-life flex-route transit service is employed to construct the SO problem, and the optimization results show that the proposed algorithm can improve the performance of flex-route transit services under unexpectedly high demand levels.

ARTICLE HISTORY
Received 15 August 2022
Accepted 23 March 2023

KEYWORDS
On-demand transportation; flex-route transit service; meeting point locations; Kriging-based global optimization method

1. Introduction

In recent decades, continued social development has resulted in massive low-demand areas, such as low-density suburban areas or sparse rural areas. This is a massive challenge for public transit systems to provide cost-efficient service and customized service in these areas. Traditional fixed-route transit services are considered inappropriate because of their rigid operating mode and the low and scattered travel demands of these areas. Pure demand responsive transit services can satisfy personal door-to-door demands; however, most of the time cost is unacceptable. At present, the most suitable transit services in these areas are flexible transit services, which combine both the cost efficiency of fixed-route transit services and the flexibility of pure demand responsive services.

Among many flexible transit services, the flex-route transit service is the most popular (Koffman 2004; Potts et al. 2010). Usually, it runs on a fixed route following a rapid timetable. Meanwhile, if someone customizes his or her personal door-to-door travel demand through dial-a-ride systems and the on-demand request is accepted, the base route is deviated to complete this request. Therefore, it can be regarded as an on-demand transportation service that is suitable in low-density suburban areas. According to practical experiences, the flex-route transit service is more attractive than the traditional fixed-route transit service (Becker, Teal, and Mossige 2013) and more cost-efficient than demand-responsive services in low-demand areas (Fittante and Lubin 2015).

CONTACT Jinjun Tang jinjuntang@csu.edu.cn Smart Transportation Key Laboratory of Hunan Province, School of Traffic and Transportation Engineering, Central South University, Changsha 410075, People's Republic of China

As an emerging on-demand transportation service, the flex-route transit service generally completes the passengers' requests at the exact locations they reserved. However, in low-demand areas, travel demand is often uncertain. The unexpectedly high-demand level led by uncertain travel demand will considerably improve the rejection rate of the flex-route transit service and further impact its service performance. Zheng, Li, et al. (2019) introduced meeting points into the flex-route transit service and proposed a new mode of flex-route transit, which is the flex-route transit with meeting points. This strategy preset meeting points among the service area, and the passengers can be picked up and dropped off either at their reserved locations or at the meeting points. Moreover, this strategy can be accomplished with smart personal devices and mobile internet.

Introducing the meeting point can benefit the flex-route transit services; however, the locations of meeting points will substantially influence the performance of this strategy. Therefore, the optimal locations of meeting points are the key issues that need to be studied.

Facing the aforementioned challenge, this study proposes a Kriging-based optimization method for the optimal location selection of meeting points in a flex-route transit system. The contributions of this study include the following:

(1) The locations of meeting points are essential to the performance of the flex-route transit system, especially under unexpected high-demand level. How to determine suitable meeting points locations is the key step to enhance performance of the flex-route transit system. To end of this, this study aims to solve the location optimization problem of the meeting points.
(2) Considering the travel demand uncertainty, the meeting point locations problem is modelled as a simulation-based optimization model based on Monte Carlo simulation. This method can obtain more realistic solutions, compared with analytical mathematical optimization model constructed in the deterministic environment.
(3) The simulation-based optimization problem is a type of computationally expensive problem. To solve the simulation-based optimization problem efficiently, a Kriging-based global optimization method using a Pareto-based multipoint sampling strategy (KGO-PS) is proposed. The numerical and simulation experiments demonstrate its effectiveness.

The remainder of this article is organized as follows: Section 2 reviews some related works. Section 3 presents the simulation-based optimization model of meeting point locations. Section 4 proposes the KGO-PS method and tests its performance through some typical benchmark functions. Section 5 studies simulation experiments based on a real-life flex-route transit line. Finally, some important conclusions and plans for future work are presented in Section 6.

2. Literature review

2.1. The operational service capability optimization strategies of the flex-route transit services

In most studies, the travel demand is assumed to be low and predictable (Qiu, Li, and Haghani 2015; Chen and Nie 2017a; Chen and Nie 2017b; Quadrifoglio, Dessouky, and Palmer 2007; Quadrifoglio, Dessouky, and Ordóñez 2008). However, in low-demand areas, the travel demand is usually uncertain. The unexpected high-demand level led by this uncertainty will cause a negative impact on system reliability (Farwell and Marx 1996) and restrict the wide application of flex-route transit service (Velaga et al. 2012; Potts et al. 2010).

To resolve this, some operational service capability optimization strategies were proposed to improve the operational mode of the flex-route transit services and further promoted the performance of flex-route transit services under unexpectedly high demand levels; in this way, the negative impact led by uncertain travel demand can be reduced. At present, three strategies exist: Qiu, Li, and Zhang (2014) proposed a dynamic station strategy. In this strategy, accepted pick-up/drop-off locations are

defined as temporary stations, which are provided to unaccepted passengers for their pick-up/drop-off. Zheng, Li, and Qiu (2018) proposed a slack arrival strategy; this method changes the distribution of slack time between different segments by setting a threshold. With the development of information science, the meeting-point-based mode is widely used in on-demand transportation services (Aïvodji et al. 2016; Czioska, Mattfeld, and Sester 2017; Qian et al. 2017). As an emerging on-demand transportation service, introducing meeting points into the flex-route transit service can considerably improve its performance under unexpectedly high-demand levels (Zheng, Li, et al. 2019). However, their work only deployed the meeting point locations randomly while overlooking the importance of the meeting point locations. Moreover, according to Qiu, Li, and Zhang (2014), the simulation model can reproduce the complex operational process of the flex-route transit system better than the analytical mathematical model. Therefore, the meeting point location selection must be modelled as an SO problem, which uses a simulation model to capture the sophisticated relationship between meeting point locations and the evaluation indicators of the flex-route transit system.

2.2. Simulation-based optimization (SO) problem

The SO problem is essentially a special optimization problem whose objective functions (or constraints) are computed through simulations. It can reproduce the complexities real life better than an analytical mathematical model, and solving it can obtain a more realistic programme.

At present, SO problems are widely constructed for describing the real-life conditions of transportation services (Huang, Sun, and Zhang 2022; Hao, Song, and He 2022; Xiong et al. 2018; Gkiotsalitis and Cats 2019; Kim et al. 2022; Liu et al. 2022). For example, Schmaranzer, Braune, and Doerner (2020) proposed a headway optimization model based on the simulation of urban mass rapid transit networks. The SO problem was a biobjective optimization problem, which contained cost reduction and service level improvement. Liu et al. (2017) designed a simulation-based optimization problem for the two-echelon vehicle routing problem based on stochastic demands. Chávez et al. (2017) studied supply chains and constructed a biobjective SO problem that minimized the stochastic transportation time and the deterministic freight rate. Chen et al. (2018) considered the travel time variability in a network, and the congestion-pricing problem with reliability maximization was modelled as an SO problem.

SO problems are tricky but common in real life engineering applications. There are some drawbacks to solving SO problems:

(1) The computation of the objective function value of the SO is based on the sophisticated simulation process (i.e. 'Black-box' property) and not on the analytical mathematical model. This means that the gradient of the SO model is hard to obtain, which leads to inappropriate gradient-based mathematical optimization methods (Winston, Venkataramanan, and Goldberg 2003).
(2) The computational cost and the number of function evaluations are high when solving the SO problems. Therefore, metaheuristics algorithms, such as the genetic algorithm and Tabu search, which depend on random and extensive exploration in the whole design domain, are difficult to be applied widely (Zheng, Xue, et al. 2019).

Therefore, essentially, the SO problem is a type of expensive black-box problem. The surrogate-based global optimization is an efficient way that (Koullias and Mavris 2014) has received increasing attention in recent years. Common surrogate models include the response surface, Kriging model, radial basis function, and least square support vector regression. The core of surrogate-based global optimization is to use surrogate models to predict new-step solutions based on known sampling points through constant iterations; in this way, a relatively optimal area can finally be determined.

2.3. Infill sampling strategy in surrogate-based global optimization

In the process of surrogate-based global optimization, the core is the infill sampling strategy. The step is to obtain new potential sampling points to renew the surrogate models in each iteration.

After several iterations, the optimization process may reach some important regions, such as the small neighbourhood around the global optimum (Long et al., 2015). Over the past few decades, many infill sampling strategies have been proposed for surrogate-based global optimization. According to the number of sampling points in each iteration, they can be generally divided into two types: single-point infill sampling strategy and multipoint infill sampling strategy. The single-point infill sampling strategy adds only one point in each iteration. The most well-known is the efficient global optimization (EGO), which is based on the expected improvement (EI) strategy; it selects the sampling point that has the maximized EI function values based on the Kriging model (Jones, Schonlau, and Welch 1998). The EI function considers both global exploration and local exploitation, and thus, it can lead the optimization process efficiently. A bumpiness-based infill sampling strategy was proposed for application in the RBF model (Gutmann 2001), and the strategy selects the point with the least bumpiness. Apart from this, Regis and Shoemaker (2007) constructed a candidate sampling strategy through the predicted value and the minimum distance to the known sampling points to select the best point in a group of candidates.

However, it should be noted that the single-point infill sampling strategy is not efficient enough and is unsuitable for parallel computing for high-performance computers. Therefore, the multipoint infill sampling strategy, which selects multiple sampling points in each iteration, is suitable for parallel computing and has received increasing attention (Haftka, Villanueva, and Chaudhuri 2016). An effective infill sampling strategy must consider the balance between global exploration and local exploitation (i.e. sampling points obtained through both global searching and local searching). According to Chung, Park, and Choi (2018), the criterion that obtains sampling points balancing exploration and exploitation can be divided into two types: (1) Using a searching function that contains both global exploitation and local exploitation (such as the EI function or the *P*-EI (Xing, Luo, and Gao 2020) function) to obtain new sampling points. (2) Using multiple search functions, some only represent global exploration (such as the prediction error function of Kriging), and others only represent local exploitation (such as the prediction value function of Kriging). For example, Viana, Haftka, and Watson (2013) considered the nature that balances the exploitation and exploration of the EI function and extended the EI to more surrogate models. In this method, the prediction error of the Kriging model is shared with other surrogate models to help construct the EI. However, this method has its drawbacks: the number of sampling points in each iteration will be restricted to the number of surrogate models. Dong et al. (2016) proposed a multistart sampling strategy in reduced space based on the Kriging model. This strategy optimizes the prediction function of Kriging using a multistart optimization algorithm. To balance exploration and exploitation, it uses the Kriging prediction error to explore unknown areas. Then, Dong et al. (2019) proposed a surrogate-assisted global optimization using a Pareto-based sampling strategy. This algorithm constructs a multiobjective optimization model, which contains QRS prediction, RBF prediction, Kriging prediction and the Kriging error, and solves it to obtain a set of sampling points balancing exploration and exploitation. However, the strategy has two disadvantages: (1) three objectives represent local searching, and only one represents global searching. Hence, most of the sampling points may pay more attention to local searching. (2) The information of global searching is completely from the Kriging; when the sampling points are selected from more on QRS and RBF, the balance between exploration and exploitation is fragile. Li, Bing, and Yang (2022) employed the EI function and proposed two sampling functions to obtain new sampling points balancing exploration and exploitation. However, this method selects sampling points that pay more attention to local exploitation and lack the means to jump out of the local valley.

In this work, a Kriging-based global optimization method using a Pareto-based multipoint sampling strategy (KGO-PS) is proposed. This method provides a novel sampling mechanism for creating a unique balance between global exploration and local exploitation based on a type of extended EI function (i.e. the *P*-EI function). The KGO-PS constructs a biobjective optimization problem based on the *P*-EI function, whose two objective functions represent global exploration and local exploitation, and solves it by the multiobjective evolutionary algorithms based on decomposition (MOEA/D). In this way, a Pareto optimal set containing multiple candidate points balancing

exploration and exploitation can be obtained. Then, some potential sampling points will be selected from the Pareto optimal set according to the probability of the improvement criterion. Moreover, reduced-domain-based local sampling and global sampling are proposed to assist the KGO-PS. Finally, the KGO-PS is applied to 11 benchmark functions and simulation experiments based on a real-life flex-route transit service. The optimization results demonstrate that the KGO-PS outperforms other counterparts, which is more reliable and effective in solving expensive black-box problems.

3. Problem description

In this article, considering the uncertainty of the passengers' travel demands, the meeting point locations problem is modelled as a simulation-based optimization problem. Then, a Kriging-based global optimization method using a Pareto-based multipoint sampling strategy (KGO-PS) is proposed to effectively solve the problem. The methodology framework can be seen in Figure 1.

In this section, the simulation-based optimization model for meeting point location problem is introduced. The proposed KGO-PS algorithm will be presented in Section 4.

3.1. Flex-route transit system with meeting points

The mode of flex-route transit with meeting points (FRT-MP) (see Figure 2) was introduced by Zheng, Li, et al. (2019). In general, the FRT-MP system can be assumed to be a rectangle with length L and width W. The operational mechanism of the flex-route transit service with meeting points can be described (see Figure 2) as follows: The bus operators will deploy some meeting points that have their fixed and suitable locations into the service area before real life applications, according to the land use, questionnaire surveys or operation planning methods. Then, the passengers can be picked up or dropped off either at their reserved locations or at meeting points that are located in their accepted walking distance. The vehicle runs according to the base route following a rapid timetable; it must drive from one

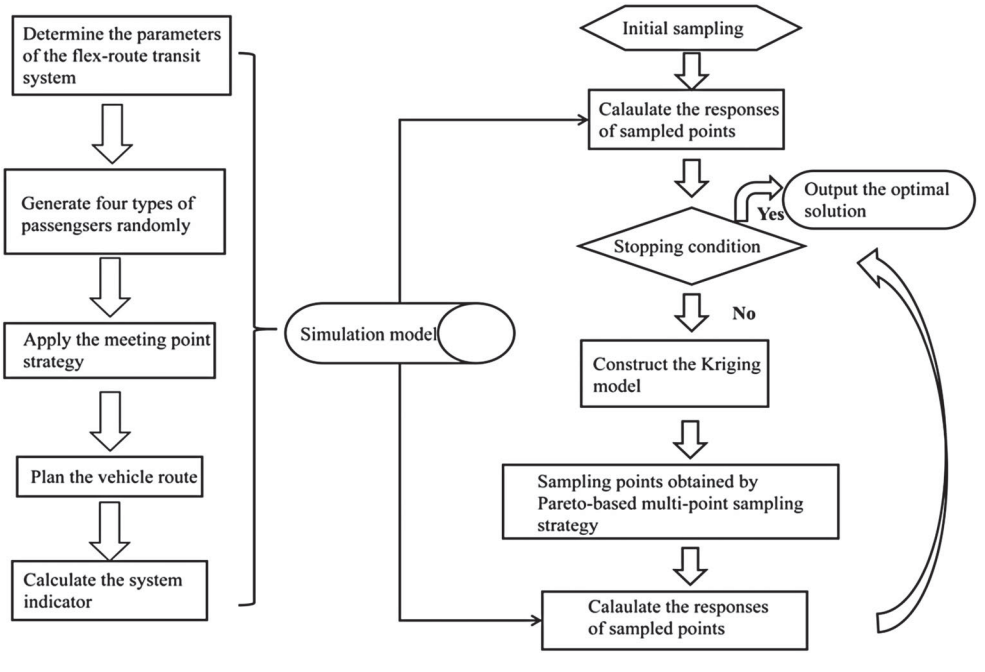

Figure 1. The methodology framework of the meeting point locations problem.

terminal checkpoint to another after visiting all intermediate checkpoints (the black rectangle). If there is a request outside the base route, in the case of meeting the timetable of two adjacent checkpoints, the bus will deviate the base route to satisfy the request (the green circle). Otherwise, the request will be rejected (red circle).

The passengers of the flex-route transit service can be divided into four types according to the locations of their requests:

Type I: Pick-up and drop-off points, both not at checkpoints (deviated request outside checkpoints).
Type II: Pick-up points at checkpoints, not drop-off points (deviated request outside checkpoints).
Type III: Drop-off points at checkpoints, pickup points at (deviated request outside checkpoints).
Type IV: Pick-up and drop-off points both at checkpoints (nondeviated requests outside checkpoints).

The meeting point strategy can reduce the vehicle detour and improve the performance of the flex-route transit services under unexpectedly high demand levels effectively. Moreover, with the development of smart personal devices and mobile internet, passengers can complete their payments and reservations and obtain pick-up/drop-off location information through online digital platforms. In this background, flex-route transit services with meeting points are suitable and promising.

According to Zheng, Li, et al. (2019), during real life operations, the locations of meeting points should be conducted appropriately. Therefore, selecting a suitable meeting point location is an important research direction.

3.2. Simulation model of the flex-route transit system with meeting points

According to Zheng, Li, et al. (2019), the operational process of the flex-route transit service with a meeting point strategy (FRT-MP) (see Figure 3) can be described as follows: There are several meeting points in the service area. The passengers will reserve their pick-up and drop-off locations by the online

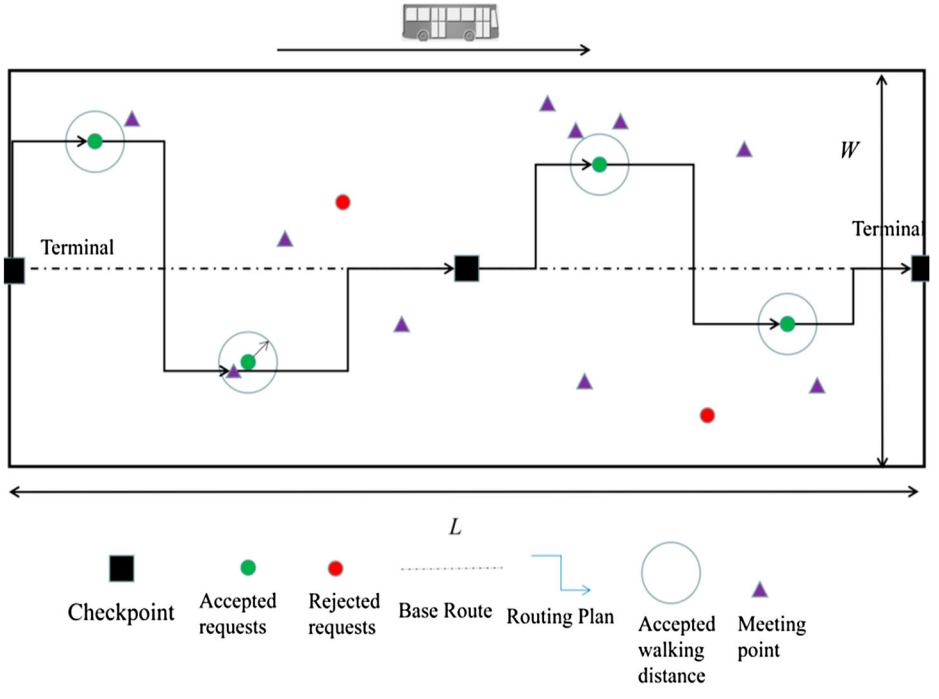

Figure 2. Flex-route transit service with meeting points.

reservation system. After receiving the requests of the passengers, the reservation system plans the transit route according to the rule of the meeting point (see Section 3.1) and the passengers' reserved requests. Considering that the passengers' travel demands are uncertain in real life, a simulation model based on Monte Carlo simulation is constructed to reproduce the FRT-MP operational process through the following steps:

Step 1. Determine the research basis, including service area, timetable, meeting points and other operational parameters.
Step 2. Determine whether the preset iteration number of the Monte Carlo Simulations is met. If yes, go to Step 3; otherwise, go to Step 6.
Step 3. Approximate the demand generation and obtain passengers' pick-up and drop-off requests.
Step 4. Use the insertion heuristic algorithm based on the first-come, first-served policy (Qiu, Li, and Zhang 2014; Zheng, Li, and Qiu 2018) to plan the vehicle path.

The parameters of the flex-route transit system are displayed as follows:
P: The number of checkpoints,
FS: Set of all non-checkpoints,
MP: Set of all meeting points,
PS: Set of the stations at the checkpoints, $PS = \{1, 2, \ldots, P\}$,
DT_p: Scheduled departure time of each checkpoint, $p \in PS$,
RP: Set of all passengers' request stations, $RP = RP_{\text{TypeI}} \cup RP_{\text{TypeII}} \cup RP_{\text{TypeIII}} \cup RP_{\text{TypeIV}}$,
$|RP|$: Number of all passengers' request stations,
Tdr: Dwell time at non-checkpoints,
Tdf: Dwell time at checkpoints,
V_b: The speed of vehicle,
V_w: The speed of passengers,
SS: Set of nodes in the flex-route transit system network, $SS = PS \cup FS \cup MP$,
AP: Set of all accepted requests,
AS: Matrix of arcs of all possible stations, $AS = SS^2$,

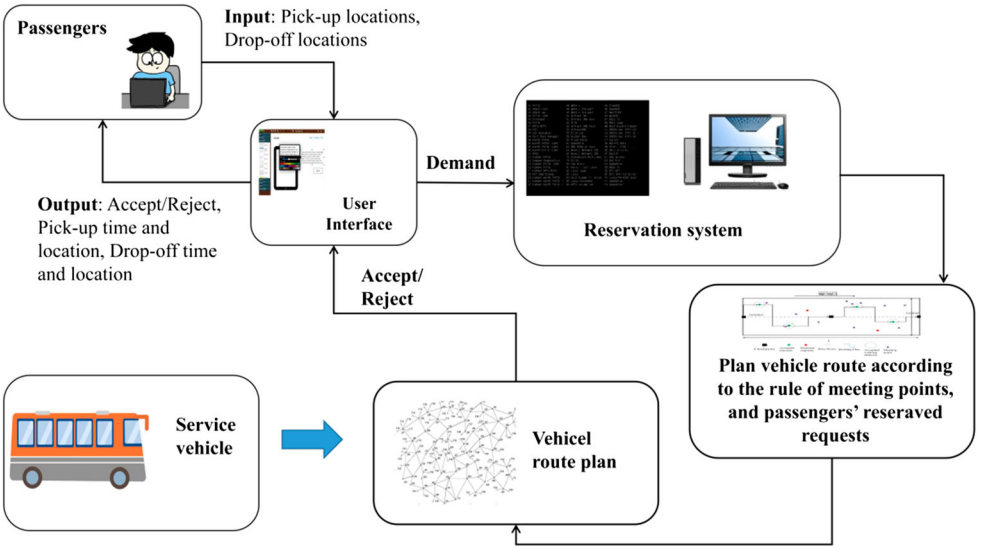

Figure 3. The operational process of the flex-route transit system with meeting points strategy.

d_{ij}: Distance from node i to node j, $\forall\, i, j \in SS$,
x_{ij}: $x_{ij} = 0, 1$, if the request: i to j is accepted, $x_{ij} = 1$; else, $x_{ij} = 0$,
y_i: $y_i = 0, 1$, if the node i is accepted, $y_i = 1$; else, $y_i = 0$,
p_k: pick-up time of request k,
d_k: drop-off time of request k,
T_r: Vehicle riding time in a trip,
M: The fleet size of the flex-route transit system,
O_P: Operating cost per vehicle,
K: All passengers' walking time,
W_K: Walking time cost per passenger,
A: All passengers' waiting time,
W_A: Waiting time cost per passenger,
R: All passengers' riding time,
W_R: Riding time cost per passenger,
I: All passengers' idle time,
W_I: Idle time cost per passenger.
Then, the route plan model can be defined as follows:

$$\text{Min}: O_P * M * T_r + W_K * K + W_A * A + W_R * R + W_I * I \tag{1}$$

Subject to:

$$T_r = \sum_{i,j \in PS \cup FS \cup MP} x_{ij} d_{ij} / V_b \tag{2}$$

$$K = \sum_{i \in AP} \sum_{j \in AP \cup PS} x_{ij} d_{ij} / V_w \tag{3}$$

$$A = \left(\sum_{i \in FS} y_i * Tdr + \sum_{i \in PS} y_i * Tdf \right) \tag{4}$$

$$R = \sum_{k \in AP} (d_k - p_k) \tag{5}$$

$$I = \sum_{p \in P-1} DT_p - T_{rp} \tag{6}$$

$$\sum_{j \in SS} x_{1j} = 1 \quad \sum_{j \in SS} x_{j1} = 0 \tag{7}$$

$$\sum_{j \in SS} x_{Pj} = 0 \quad \sum_{j \in SS} x_{jP} = 1 \tag{8}$$

$$\sum_{i,j \in SS/\{1,P\}} x_{ij} = \sum_{i,j \in SS/\{1,P\}} x_{ji} = y_i \tag{9}$$

$$x_{ii} = 0 \quad \forall i \in SS \tag{10}$$

$$DT_p - T_{rp} \geq 0, \quad \forall p \in PS \tag{11}$$

The formulation (1) is the system evaluation indictor in this trip. The formulation (2–6) is the vehicle riding time, passengers' walking time, waiting time, riding time, and idle time. The formulation (7) represents the outgoing/incoming degree of the first checkpoint are 1/0. The formulation (8) represents the outgoing/incoming degree of the final checkpoint are 0/1. The formulation (9) represents: if the node i is accepted, its outgoing/incoming degree are both equal to 1; else, they are equal to 0. The

formulation (10) represents there is no self-connection of the node *i*. The formulation (11) is the core constrain, which represents the vehicle needs to follow the timetable of each checkpoint.

Step 5. Obtain specific travel data for each passenger and vehicle, and then return to step 2:
Step 6. Calculate the total system performance indicator:

$$F = \sum_{l=1}^{N} (O_P * M * T_{rl} + W_K * K_l + W_A * A_l + W_R * R_l + W_I * I_l)/N \tag{12}$$

where F is the performance indicator of the flex-route transit system, which represents the expected cost of the system under different travel demands (Zheng, Li, et al. 2019). N is the pre-set number of travel demand generations (i.e. The number of iteration/Monte Carlo Simulation), which is set as 10,000 in this article. O_p is the operating cost per vehicle, M is the fleet size of the system, and T_{rl} is the vehicle riding time of the flex-route transit service in the l-th iteration. W_K is the walking time cost per passenger, and K_l is the walking time of all passengers in the l-th iteration. W_A is the waiting time cost per passenger, and A_l is the walking time of all passengers in the l-th iteration. W_R is the riding time cost per passenger, and R_l is the riding time of all passengers in the l-th iteration. W_I is the idle time cost per passenger, and I_l is the idle time of all passengers in the l-th iteration.

According to Koffman (2004), most flex-route transit systems generally have a long headway over half an hour. Hence, it is worth noting that it is more practical for passengers using flex-route transit services to book specific trips based on the transit timetable instead of specifying a narrow time frame for pick-up and drop-off services (Zheng, Li, et al. 2019).

Moreover, some adopted assumptions in previous studies (Qiu, Li, and Zhang 2014; Zheng, Li, and Qiu 2018; Zheng, Li, et al. 2019) were employed in this study: (1) To facilitate analysis, only one of the up and down directions is considered. (2) Passengers will arrive on time according to the pick-up time set in advance by the reservation system without considering vehicle delay. (3) Passengers who are rejected walk directly to their destination or walk to the nearest checkpoint. (4) The vehicle drives straight in the X or Y direction.

3.3. Simulation-based optimization problem

The meeting point locations problem, considering the uncertainty of passengers' travel demand, can be described as follows: In the service area, some meeting points are preset in advance, and their locations are fixed with station boards. The passengers' requests are unknown before they make a reservation with the reservation system. After the requests are submitted, the reservation system will plan the vehicle route according to the meeting point locations and passengers' requests. Then, the system cost can be calculated. Because the meeting point location optimization for planners appears before the transit operation, considering the uncertainty of the passengers' demand, we need the optimal meeting point locations, which can lead to the expected system cost minimization under different massive reservation request scenarios.

Here, the simulation-based optimization model of determining optimal meeting points is introduced. The objective function is the expected system cost function (F). The constrained condition is the expected passenger acceptance rate (RE). The simulation-based optimization model is defined as:

$$\min : F(MP) = \sum_{l=1}^{N} (O_P * M * T_{rl} + W_K * K_l + W_A * A_l + W_R * R_l + W_I * I_l)/N \tag{13}$$

$$s.t. \quad RE = e \tag{14}$$

$$\text{Design Variables} : 0 \le MP_{xm} \le L; 0 \le MP_{ym} \le W; m \in MP \tag{15}$$

Here, F is the expected system cost function, which is calculated through the simulation model in Section 3.2. RE is the expected rejection rate of the flex-route transit service, which is also calculated through the simulation model in Section 3.2. ε is a threshold, it is set as the expected rejection rate value calculated through the simulation model, which is under the condition that the meeting points locations are unoptimized and randomly generated. The MP_{xm} and $MP_{ym}$are the design variables of the simulation-based optimization problem. MP_{xm} is the coordinate pair of the meeting points along the X axis, and $MP_{ym}$is the coordinate pair of the meeting points along the Y axis. L is the length of the service area of flex-route transit, and W is the width of the service area of flex-route transit. MP is the vector of the meeting points.

4. Solution approach

The meeting point location problem with uncertainty is modelled based on the Monte Carlo simulation, which is a simulation-based optimization (SO) problem. The SO is a type of expensive problem (i.e. The calculations of objective functions are computationally time-consuming). The Kriging-based global optimization (KGO) method is efficient in solving expensive problems. In this article, a Kriging-based global optimization method using a Pareto-based multipoint sampling strategy (KGO-PS) is proposed to solve the SO problem. The process of the KGO-PS is introduced as follows:

4.1. Kriging and P-EI function

The Kriging model is a type of surrogate model that is good at modelling multimodal and nonlinear problems. The specific details can be seen in (Sacks et al. 1989).

The expected improvement (EI) function is the most famous searching function based on the Kriging model and was first proposed by Jones, Schonlau, and Welch (1998). After obtaining a Kriging model, we suppose the minimal value of all evaluated points is $y_{\min}$. The expected value of an unobserved point relative to $y_{\min}$ can be written as:

$$E[I(x)] = [(y_{\min} - y(x))]F\left(\frac{y_{\min} - y(x)}{s(x)}\right) + s(x)f\left(\frac{y_{\max} - y(x)}{s(x)}\right) \tag{16}$$

where x is a sampling point in the design space. $y(x)$ is the Kriging predicted value of sampling point x, and $s(x)$ is the predicted Kriging standard deviation of sampling point x. Φ and φ are the cumulative distribution function and probability density function of the standard normal distribution, respectively. Based on the EI function, Xing, Luo, and Gao (2020) proposed an extended version of EI, which is the P-EI function. The P-EI function adds a parameter P to the traditional EI function to enhance the searchability for other peaks of the EI function. The P-EI is shown as follows:

$$E_P[I(x)] = [(y_{\min} - y(x))]\Phi\left(\frac{y_{\min} - y(x)}{P * s(x)}\right) + P * s(x)\varphi\left(\frac{y_{\min} - y(x)}{P * s(x)}\right) \tag{17}$$

where P is an artificially predefined parameter and is more than 0, which is a drawback of the P-EI function because its suitable value has not been proven by strict mathematical deduction. Therefore, referring to the test example of Xing, Luo, and Gao (2020) and their conclusion, the values of parameter P in this article are defined as 1, 2 and 3.

Due to $P > 0$ and $s(x) \geq 0$, learning from the deduction of Feng et al. (2015) and Sobester, Leary, and Keane (2005), some features of the P-EI function can be concluded, and the P-EI function is composed of two terms:

$$P_1 = [(y_{\min} - y(x))]F\left(\frac{y_{\min} - y(x)}{P * s(x)}\right) \tag{18}$$

$$P_2 = P * s(x)f\left(\frac{y_{\min} - y(x)}{P * s(x)}\right) \tag{19}$$

The first term P_1 reflects the local exploitation. Conversely, the second term P_2 reflects global exploration. The proving process is displayed in Appendix A. Therefore, using the *P*-EI function for global optimization is efficient because the *P*-EI balances both global exploration and local exploitation. However, the *P*-EI function gives equal weight to both exploration and exploitation. Hence, it may only carry out either local searches or global searches sometimes. In the 'Appendix B' section, an example is applied to demonstrate the disadvantage of the *P*-EI function and display our motivation.

4.2. Pareto-based multipoint sampling strategy

For designing a Kriging-based global algorithm, sampling points that balance global exploration and local exploitation can be considered promising (Zhan, Qian, and Cheng 2017a). To end this and target the disadvantage of *the P*-EI function, this article proposes a Pareto-based multipoint sampling strategy.

4.2.1. Sampling points obtained by biobjective optimization

First, the concept of 'Pareto optimality' must be introduced, considering a biobjective optimization problem:

$$\min : f = \{f_1(x),\ f_2(x)\} \tag{20}$$

$$\text{subject to} : x = \{x^1,\ x^2,\ \ldots,\ x^n\} \tag{21}$$

Then, considering two vectors, x^1 and x^2, if the following condition is met, it can be concluded that x^2 dominates x^1 or $x^1 < x^2$.

$$f_i(x^1) \geq f_i(x^2), \quad \forall\, i;\ f_i(x^1) > f_i(x^2), \quad \exists i, i = 1, 2 \tag{22}$$

If there are no solutions that can dominate solution x in the whole design space, solution x can be called the Pareto optimal solution. A set of Pareto optimal solutions is called the Pareto optimal set, and their corresponding objective function values compose the Pareto front. The aim of multiobjective optimization is to obtain a reliable Pareto optimal set.

Based on the above, a spontaneous idea is that by solving a biobjective optimization problem, whose objectives represent global exploration and local exploitation, a Pareto optimal set containing candidate sampling points with different weights between exploration and exploitation can be obtained. In this work, the biobjective optimization problem (see Formulations 25, 26 and 27) is constructed based on *P*-EI functions. Consider the following six search functions:

$$P_1 = [(y_{\min} - y(x))]F\left(\frac{y_{\min} - y(x)}{P * s(x)}\right), \quad P = 1, 2, 3 \tag{23}$$

$$P_2 = P * s(x) f\left(\frac{y_{\min} - y(x)}{P * s(x)}\right), \quad P = 1, 2, 3 \tag{24}$$

When the values of *P* are different, P_1 and P_2 with $P = 1, 2, 3$ will have idiographic advantages in solving different problems. Generally, selecting the most suitable searching function for a particular problem is difficult. Because of the black-box properties of most simulation-based problems, the problem characteristics are difficult to capture in advance. A way to solve this problem is the integrated method (Shi, Xie, and Wang 2013), which aggregates different searching functions into one integrated function. The aim of the integrated method is to consider and balance all search functions that are aggregated and implement search capabilities for each aggregated search function as much as possible. In this way, the impact of selecting an unsuitable search function can be reduced. In this work, the integrated method in the work (Li, Bing, and Yang 2022) is employed. The two integrated objectives and the biobjective optimization problem are shown as follows:

$$O_1 = \frac{1}{q} \ln\left(\sum\nolimits_{P=1}^{3} \exp\left(-[(y_{\min} - y(x))]\Phi\left(\frac{y_{\min} - y(x)}{P * s(x)}\right)\right)/q\right) \tag{25}$$

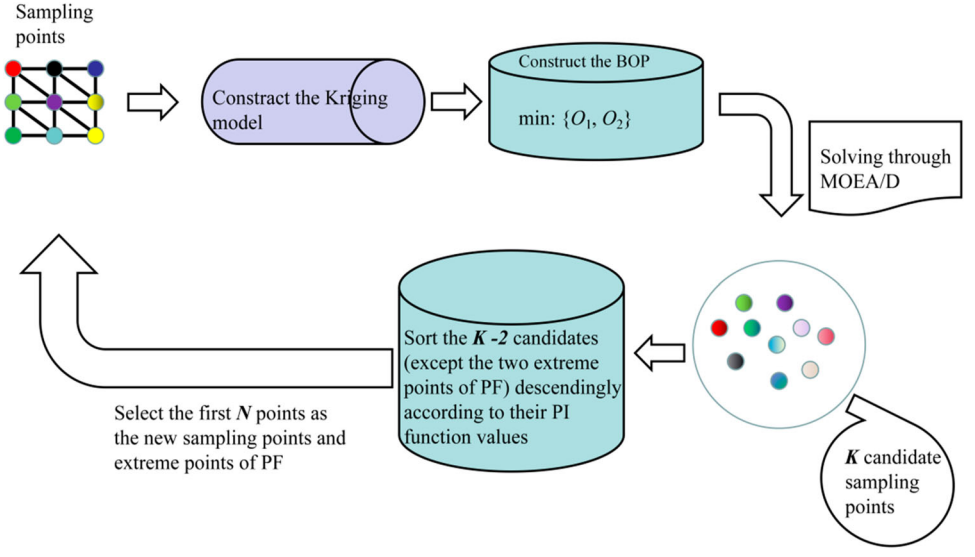

Figure 4. The process of selecting sampling points through biobjective optimization.

$$O_2 = \frac{1}{q} \ln \left(\sum_3^{P=1} \exp \left(-P * s(x) f \left(\frac{y_{\min} - y(x)}{P * s(x)} \right) \right) / q \right) \tag{26}$$

$$\min : \{O_1, O_2\} \tag{27}$$

where q is a control parameter and adopted the default value in (Li, Bing, and Yang 2022). Due to the monotonic increase in exponential and logarithmic functions, minimizing O_1 requires that each P_1 ($P = 1, 2, 3$) be as large as possible; similarly, minimizing O_2 requires that each P_2 ($P = 1, 2, 3$) be as large as possible. Therefore, O_1 represents local exploitation, and O_2 represents global exploration.

After the biobjective optimization problem is constructed, the multiobjective evolutionary algorithm based on decomposition (MOEA/D) (Zhang and Li 2007) is employed to solve it. The details of the MOEA/D can be seen in Appendix C. Then, because the two extreme points of the Pareto front represent exploration and exploitation, to balance exploration and exploitation, they will be first selected as sampling points. Finally, the probability of the improvement (PI) function (Jones 2001) is employed as the criterion to select new sampling points from the remaining candidates. The formulation of the PI function is shown as follows:

$$PI = F \left(\frac{y_{\min} - y(x)}{s(x)} \right) \tag{28}$$

The PI function has a concrete practical meaning; it represents the probability that the objective function value of an unobserved point is better than the current optimum. Hence, it is usually employed to select potential sampling points. The sampling process is shown in Figure 4:

4.2.2. Space-reduction-based greedy sampling

To further mine more precise optimal solutions, a space-reduction-based greedy sampling strategy is proposed.

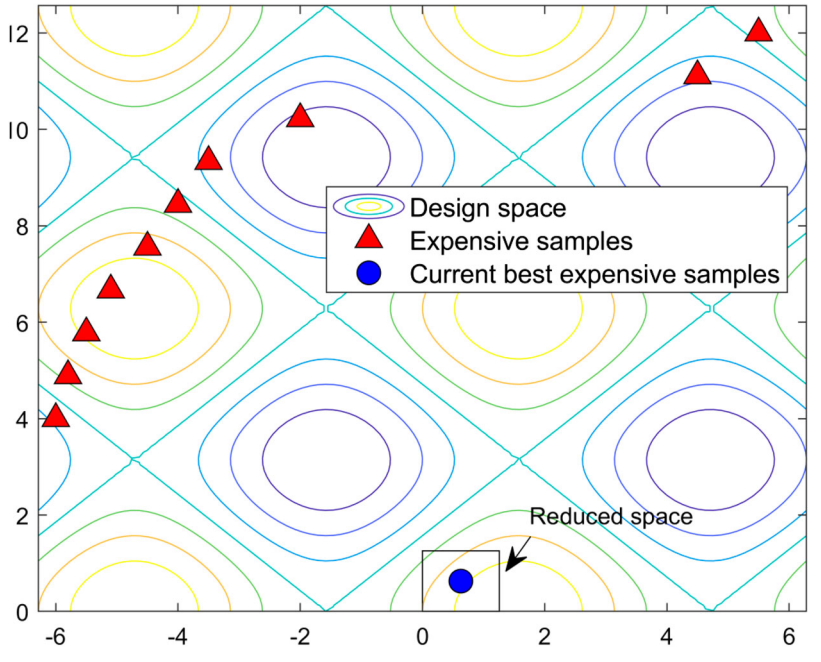

Figure 5. Reduced space obtained by Formula (29)–(30).

The space reduction technology obtains a trust region that contains possibly potential sampling points (Dong et al. 2016; Dong et al. 2018b; Gu 2021); in this way, the cost computing resource can be decreased, and the search efficiency can be improved. Generally, the reduced space (Dong et al. 2018a) is a neighbourhood of the current best point (see formulation 29–30; Figure 5) and/or a small hypercube (see formulation 31–33; Figure 6) composed of several promising points.

$$ox = \left\{ \begin{array}{ccc} [xbest_1 - e, xbest_1 + e] & \cap & [lb_1, ub_1] \\ [xbest_2 - e, xbest_2 + e] & \cap & [lb_2, ub_2] \\ [xbest_3 - e, xbest_3 + e] & \cap & [lb_3, ub_3] \\ \vdots & \vdots & \vdots \\ [xbest_{d-1} - e, xbest_{d-1} + e] & \cap & [lb_{d-1}, ub_{d-1}] \\ [xbest_d - e, xbest_d + e] & \cap & [lb_d, ub_d] \end{array} \right\} \tag{29}$$

$$\varepsilon = \delta * (ubi - lbi) \tag{30}$$

where *xbest* is the best sampled point. d is the dimension of the design space. lb_i and ub_i are the lower and upper boundaries of the i-th dimension. δ is a threshold, which is small; it is set as 0.05 in this article, according to sensitivity analysis.

$$Point^{topM} \left[\begin{array}{cccc} point_1{}^{rank1} & point_2{}^{rank1} & \cdots & point_d{}^{rank1} \quad Y^{rank1} \\ point_1{}^{rank2} & point_2{}^{rank2} & \cdots & point_d{}^{rank2} \quad Y^{rank2} \\ \vdots & \vdots & \cdots & \vdots \quad \vdots \\ point_1{}^{rankM} & point_2{}^{rankM} & \cdots & point_d{}^{rankM} \quad Y^{rankM} \end{array} \right] \tag{31}$$

$$LB_i = \min(point_i{}^{rank1}, point_i{}^{rank2}, \ldots, point_i{}^{rankM}), i = 1, \ldots, d \tag{32}$$

$$UB_i = \max(point_i{}^{rank1}, point_i{}^{rank2}, \ldots, point_i{}^{rankM}), i = 1, \ldots, d \tag{33}$$

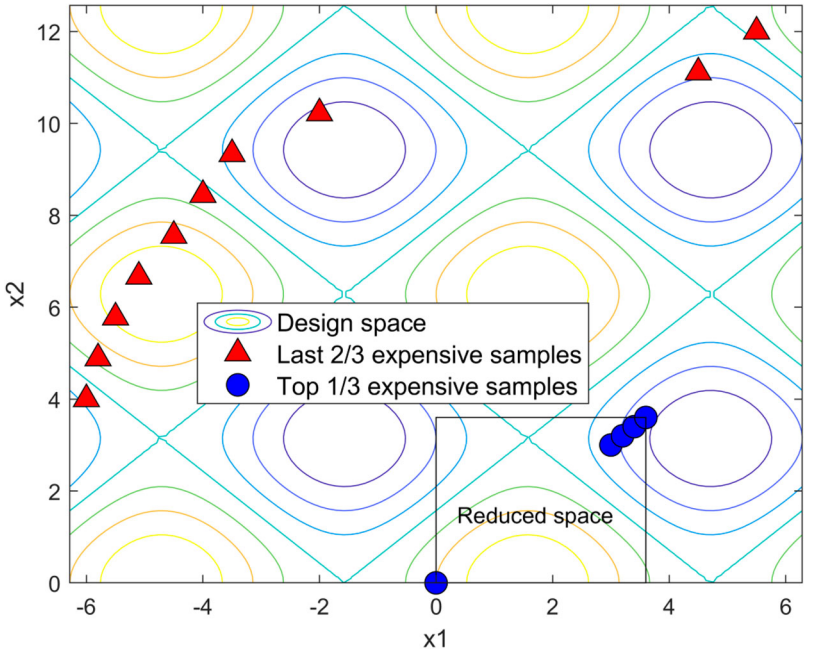

Figure 6. Reduced space obtained by Formulas (31)–(33).

where $Point^{topM}$ is the set composed of the top M most expensive samples, and M is set to 1/3 in this article. LB_i and UB_i are the lower and upper boundaries in the i-th dimension of the reduced space.

After obtaining the reduced space, two unevaluated points with the smallest Kriging prediction value are sampled in the two reduced spaces mentioned above. Then, the two points are regarded as new sampling points. Its pseudocodes are shown below:

Algorithm 1. Space-reduction-based greedy sampling

Input: The Kriging trained through all expensive samples, Expensive samples set: $S = \{S_1, S_2, \dots, S_K\}$ and their corresponding responses set: $Y = \{Y_1, Y_2, \dots, Y_K\}$, The dimension d of design space Ω, The lower and upper boundaries $[lb_i, ub_i]$ of the i-th dimension.
Output: two new sampling points $[local_1, local_2]$ through local search.
(1) Obtain the current best responses: $Y_{\min}$ in the set Y and its corresponding samples: *xbest*.
(2) Construct the reduced space 1: neighbourhood of the current best point.
Construct the reduced space 2: hypercube composed of several promising points.
Based on reduced space 1, minimizing the Kriging prediction value:
$$\text{Min: } y(x) = f^T(x)\hat{\beta} + r^T(x)R^{-1}(Y - F\hat{\beta})$$
Obtain the new sampling point: $local_1$.
(4) Based on reduced space 2, minimizing the Kriging prediction value:
$$\text{Min: } y(x) = f^T(x)\hat{\beta} + r^T(x)R^{-1}(Y - F\hat{\beta})$$
Obtain the new sampling point: $local_2$.
(5) Return $[local_1, local_2]$.

4.2.3. Exploring points with high uncertainty in promising regions

When the optimization process becomes trapped in a local valley, it will result in unnecessary costs. One of the approaches is to increase the diversity of sampling (selecting high-uncertainty points). In this section, to increase the diversity of sampling and explore the sparse area, points with high uncertainty are sampled. To avoid unnecessary computing costs, the above process is based on the promising region, which is defined as the hypercube in Section 4.2.2.

A general condition for determining whether the optimization process becomes trapped in a local valley is that the best solution in the n-th iteration is almost equal to the best solution in the $(n–n_1)$-th iteration. Hence, in this article, when the following global search condition is met, the optimization process can be considered as a local valley:

$$[Best(n) - Best(n-5)] = d \tag{34}$$

where n is the current number of iterations of the algorithm and Best(n) is the best function value evaluated in the n-th iteration. δ is a threshold, in this article, which is small, $\delta = 0.005$.

Finally, two unevaluated points with the largest Kriging prediction error are sampled in the trust reduced space, and the two points are regarded as new sampling points. Its pseudocodes are shown below:

Algorithm 2. Exploring points with high uncertainty in promising region

Input: The Kriging trained through all expensive samples, Expensive samples set: $S = \{S_1, S_2, \dots, S_K\}$ and their corresponding responses set: $Y = \{Y_1, Y_2, \dots, Y_K\}$, The dimension d of design space Ω, The lower and upper boundaries $[lb_i, ub_i]$ of the i-th dimension, The current number of iteration: n, The best function value evaluated in the n-th iteration: $Best(n)$.
Output: two new sampling points $[global_1, global_2]$ through global search.
If $Best(n) - Best(n-5) \leq 0.005$
(1) Obtain the current best responses in the set Y: $Y_{\min}$, and its corresponding samples: $xbest$.
(2) Construct the trust reduced space: hypercube composed of several promising points.
(3) Based on the trust reduced space, sampling 10000 cheap points in the reduced space $CP = \dots \{cp_1, cp_2, \dots, cp_{10000}\}$ using the Latin hypercube sampling.
(4) Obtain the top two points: global_1 and global_2 with maximized Kriging error in set CP.
(5) Return $[global_1, global_2]$.
End

4.3. The overall optimization algorithm

In this section, the flowchart (see Figure 7) and process of the proposed KGO-PS algorithm are given:

Step 1: Initial sampling using the design of the experiment (DOE) methods. The sampling set is S: $\{S_1, \dots, S_2, \dots, S_K\}$, and the objective function value of each point Y is evaluated: $\{Y_1, \dots, Y_2, \dots, Y_K\}$.
Step 2: Determine whether the stopping condition is reached. If yes, output the current optimal solution. If not, go to Step 3.
Step 3: Construct the Kriging model based on the set S and Y.
Step 4: Solving the biobjective optimization problem:

$$\text{Min}: \left\{ \frac{1}{q} \ln \left(\sum_{P=1}^{3} \exp \left(-[(y_{\min} - y(x))] \Phi \left(\frac{y_{\min} - y(x)}{P * s(x)} \right) \right) / q \right), \dots \right.$$
$$\left. \frac{1}{q} \ln \left(\sum_{3}^{P=1} \exp \left(-P * s(x) f \left(\frac{y_{\min} - y(x)}{P * s(x)} \right) \right) / q \right) \right\}$$

Step 5: Select N new sampling points $SP = \{sp_1, sp_2, \dots, sp_N\}$ from the Pareto optimal set obtained in Step 4.
Step 6: Local search in the reduced space: $\{local_1, local_2\}$.
Step 7: Determine the global search condition; if yes, global search in the reduced space: $\{Global_1, Global_2\}$.
Step 8: Add SP, $\{local_1, local_2\}$, and $\{Global_1, Global_2\}$ into S.
Step 9: Delete the repeated points in set S.

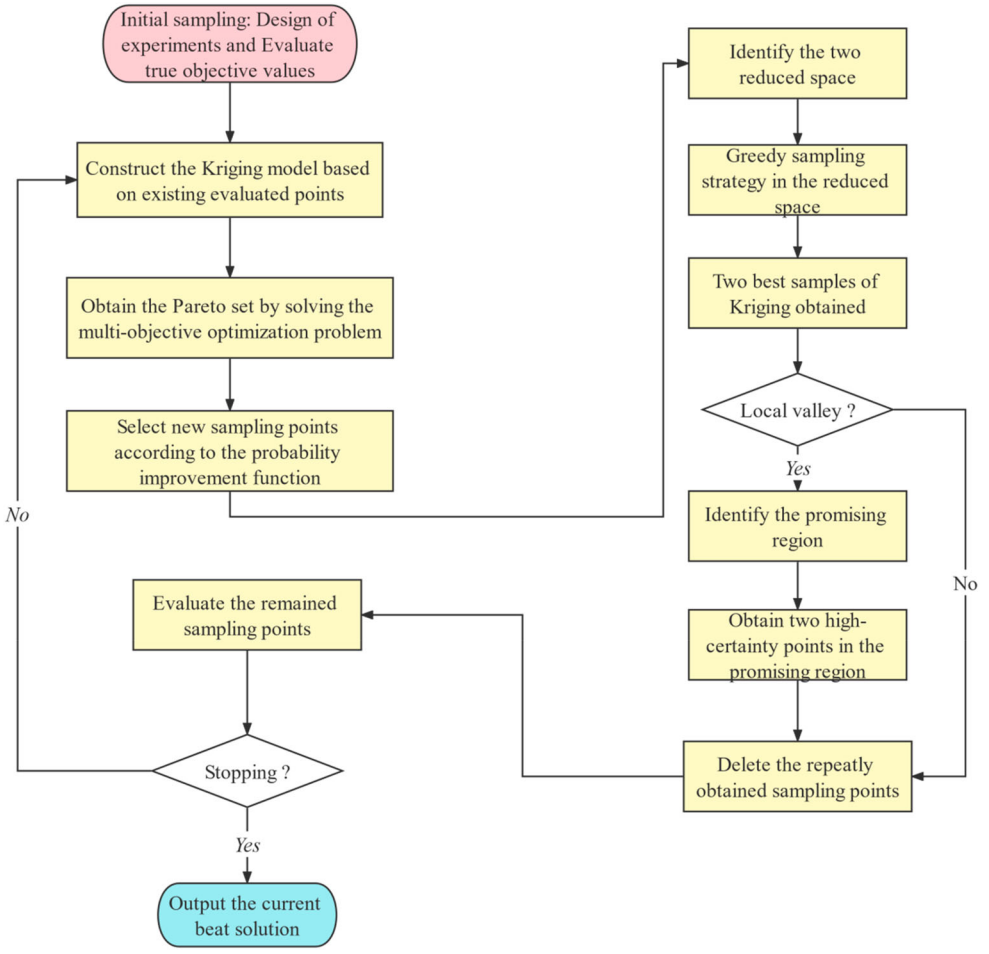

Figure 7. The flowchart of the KGO-PS algorithm.

Step 10: Evaluate the objective function value of the newly added points in S.
Step 11: Return to Step 2.

4.4. Numerical experiments to test the KGO-PS method

To verify the effectiveness and superiority, the KGO-PS is tested on 11 representative benchmark functions, including 2 lower-dimensional functions and 9 higher-dimensional functions. The details of all benchmark functions are shown in Table 1, and the formulations can be seen in the 'Appendix D' section. Then, several well-known algorithms, including EGO (Jones, Schonlau, and Welch 1998), EGO-MO (Feng et al. 2015) and MISK (Li, Bing, and Yang 2022), are employed for comparison with KGO-PS. The EGO is the most widely used Kriging-based global optimization algorithm, which is commonly applied as a competitor in comparisons. The EGO-MO and MISK are two recently extended versions of EGO that consider balancing global exploration and local exploitation. Moreover, the experimental preparation is shown below:

(1) The number of initial samplings is set to $3*d+2$ for each algorithm by using the Latin Hypercube Sampling (LHS) method, where d is the dimension of the benchmark function.

(2) To avoid unrepresentative results, 10 independent runs are applied. The optimization results are the mean values of 10 runs in this article.
(3) In these tests, the stopping condition is set to all testing algorithms: Fix the maximum number of function evaluations (NFE), and compare the mean and variance of optimal solutions (OS). The maximum NFE is set as 300 in lower-dimensional functions and 500 in higher-dimensional functions. The mean OS represents the optimization precision, while the variance OS represents the optimization robustness.
(4) The number of new sampling points *NSP* is set as 3 in this work, according to the sensitivity analysis method.

The optimization results are shown in Table E1 (see Appendix E).

In Table E1, in terms of the mean OS, the KGO-PS is considerably better than the EGO algorithm on all benchmark functions. In the variance of OS, the KGO-PS also has a smaller variance. The reason for this is that although the EGO algorithm can balance global exploration and local exploitation, it gives the same weight to them both. The EI function can be regarded as a special condition of *P*-EI ($P = 1$); hence, the balance between exploration and exploitation is fragile. In higher-dimensional problems, it is obvious that the KGO-PS has much better results because the EGO is not good at solving high-dimensional problems. In summary, the KGO-PS is more effective and reliable in solving highly multimodal and nonlinear problems than the EGO. Moreover, the KGO-PS is based on a multipoint sampling strategy, which is more in line with the needs of high-performance and multicore computers. Compared with the EGO-MO algorithm, the KGO-PS shows strong dominance in almost all benchmark functions, except for the SSF function. In terms of the mean OS, the KGO-PS shows significant precision in the F1, AK, ED10, ED12, SS, SF12, H6, F16, TF and PAF functions. This is because the EGO-MO lacks a strategy that can help it proceed with a local search in a promising region. Facing highly multimodal and nonlinear problems, it is powerless. In the variance of OS, the KGO-PS is also smaller in almost all problems. This means that the KGO-PS has advantages in stability and is more reliable.

Compared with the MISK algorithm, the KGO-PS shows strong dominance in almost all benchmark functions, except for the PAF function. In mean OS, the KGO-PS shows significant precision in F1, AK, ED10, ED12, SS, SF12, H6, F16 and SF20 functions. This is because the MISK lacks a strategy that can help it proceed with a local search in a promising region. Facing highly multimodal and nonlinear problems, it is powerless. In the variance of OS, the KGO-PS is also smaller in almost all problems. This means that the KGO-PS has advantages in stability and is more reliable.

In summary, compared with other algorithms, the proposed KGO-PS can obtain more precise optimal solutions with the same computing costs and stronger robustness. Hence, it can be concluded that the KGO-PS is more effective, which may be more suitable for solving real life problems.

Table 1. The details of the benchmark functions.

Function	Optimum	Design space	Dimension
F1	−2	[−1, 1]	2
Ackley (AK)	0	[−30, 30]	2
ED10	0	[−5, 5]	10
ED12	0	[−1, 1]	12
SS	0	[−2, 2]	10
SF12	0	[−1, 1]	12
HN6	−3.322	[0, 1]	6
Trid 6	−50	[−36, 36]	6
PAF	−45.8	[2.1, 9.9]	10
F16	25.875	[−1, 1]	16
SF20 (SSF)	0	[−10, 10]	20

Table 2. Parameter values of Line 646.

Parameter	Description	Value
L	The length of the service area	10 miles
W	The width of the service area	1 mile
M	The fleet size of the flex-route transit system	1
C	The number of checkpoints	3
D	Unexpectedly high-demand level	25 passenger/trip
V_b	The speed of the vehicle	25 miles/h
V_w	The speed of the passengers	3 miles/h
W_K	Walking time cost per passenger	\$25/passenger/h
W_A	Waiting time cost per passenger	\$15/passenger/h
W_R	Riding time cost per passenger	\$30/passenger/h
W_I	Idle time cost per passenger	\$20/passenger/h
O_p	Operating cost per vehicle	\$60/vehicle/h
Tdr	Dwelling time at on-demand request stops	0.3 min
Tdf	Dwelling time at checkpoints	1 min
T_{unit}	The predefined trip time between two consecutive checkpoints	20 min
T_r	The predefined single-trip time	40 min
$\beta_1/\beta_2/\beta_3/\beta_4$	The proportions of four types of passengers	0.1/0.4/0.4/0.1
D_{walking}	Accepted walking distance of passengers	0.5 mile

5. Case study

In this section, the KGO-PS is applied to solve the simulation-based optimization problem in Section 3. To display the effectiveness of KGO-PS, some representative algorithms are selected as competitors, including particle swarm optimization (PSO), which is a typical metaheuristic; efficient global optimization (EGO), which is the most well-known Kriging-based optimization algorithm and is widely used in engineering applications; EGO-MO and MISK, which are recent Kriging-based global optimization algorithms using a multipoint infill sampling strategy.

5.1. Parameter values in the simulation model

The simulation model of the flex-route transit service is performed through MATLAB 2020a and Line 646 in Los Angeles (see Figure 8). It was generally applied as a case study in previous works (Quadrifoglio, Dessouky, and Palmer 2007, 2008; Qiu, Li, and Zhang 2014; Zheng, Li, and Qiu 2018; Zheng, Li, et al. 2019). When it is employed as a case study, Line 646 is modelled hypothetically (see Figure 9). The flex-route transit system is composed of three checkpoints, one base route, a single service vehicle, and a service area with length L and width W. The parameters in the simulation model are given by Zheng, Li, et al. (2019) and can be seen in Table 2:

For comparison, the value of system cost function of flex-route transit system with unoptimized meeting points are set as the initial value. To avoid the contingency of the initial value, the results are calculated as the average simulation values of flex-route transit system, whose meeting points are randomly generated with 10 times. The calculated results are $F = 366.5$, while $RE = 35.73\%$.

According to Wu et al. (2021), the dimension of the expensive black-box problem is 10–30, and it can be regarded as a difficult high-dimensional optimization problem. Therefore, I should not be a number that is too large. In this article, I is set to 10, and the optimization model has 20 variables.

5.2. Optimization results

The optimization results can be seen in Table 3, and the optimization processes of PSO, EGO, MSIK, EGO-MO and KGO-PS are shown in Figures 10–12. In the actual problem, the stopping condition of each algorithm is set to NFE $>$ $NFE_{\max}$. For EGO, MISK and KGO-PS, the $NFE_{\max}$ is 500. Because metaheuristics for expensive black-box problems generally require more NFE; its $NFE_{\max}$ is set to 1000.

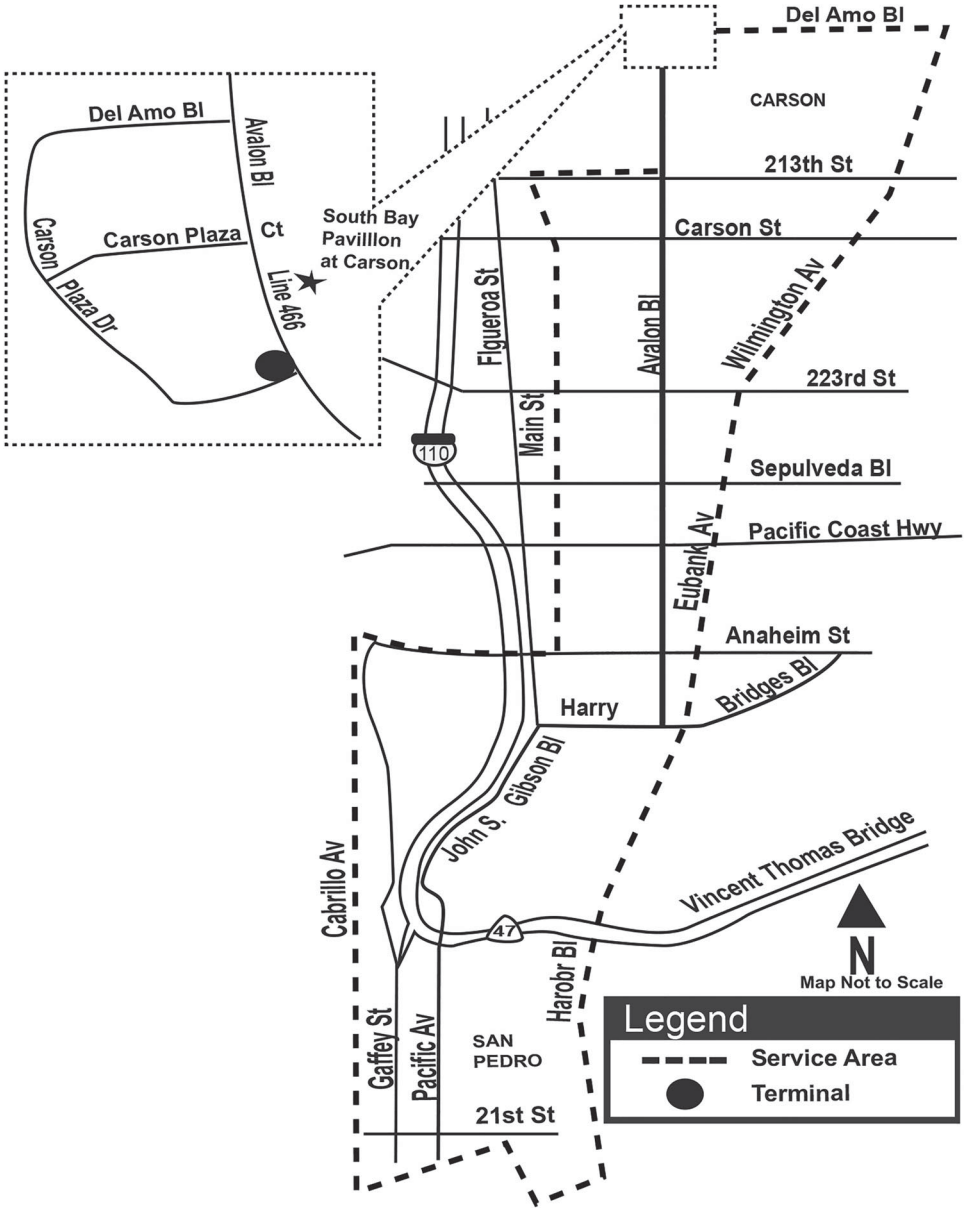

Figure 8. The schematic diagram of Line 646.

In Figure 10, the best values of PSO are taken over by EGO and KGO-PS after approximately 20 NFE. The searching process of PSO continues to gather at one value for a long time because PSO is a method of unordered search; it keeps going in the direction of letting it down. When it is in a local valley, it jumps out with unacceptable NFE. Hence, it is unsuitable for expensive black-box problems due to too many expensive computing resources. Compared with PSO, the EGO and KGO-PS can jump out the local valley using less NFE because they explore the design space based on the Kriging information and can make a unique balance between global exploration and local exploitation. Compared with EGO, KGO-PS can obtain better values after approximately 100 NFE. In addition, the consumed NFE that KGO-PS needs when it continues to gather at one value is less than EGO, which means that

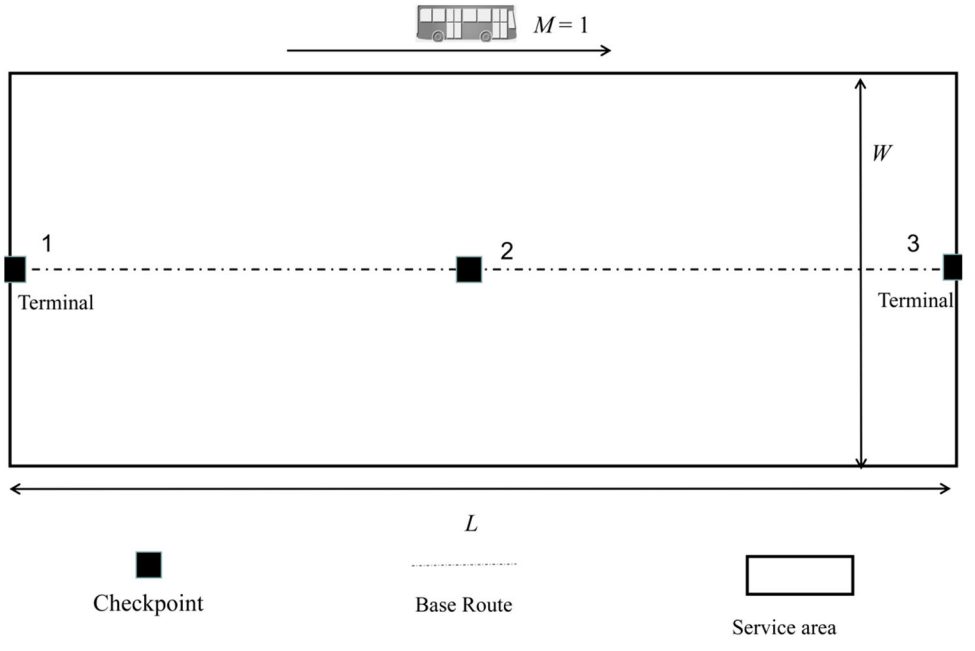

Figure 9. The hypothetical model of Line 646.

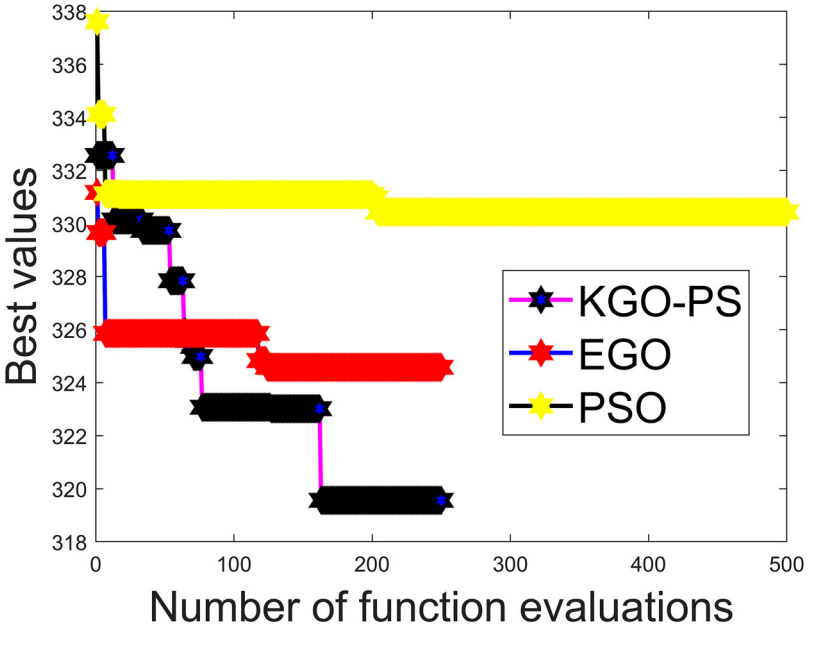

Figure 10. Iterative results based on NFE (PSO, EGO and KGO-PS).

the ability of KGO-PS to jump out of the local optimal solution is stronger than EGO. This is normal because the EI function can be regarded as a special *P*-EI, and sometimes its balance between exploration and exploitation is fragile, as mentioned above. The KGO-PS can explore the whole design space completely and find better solutions more easily.

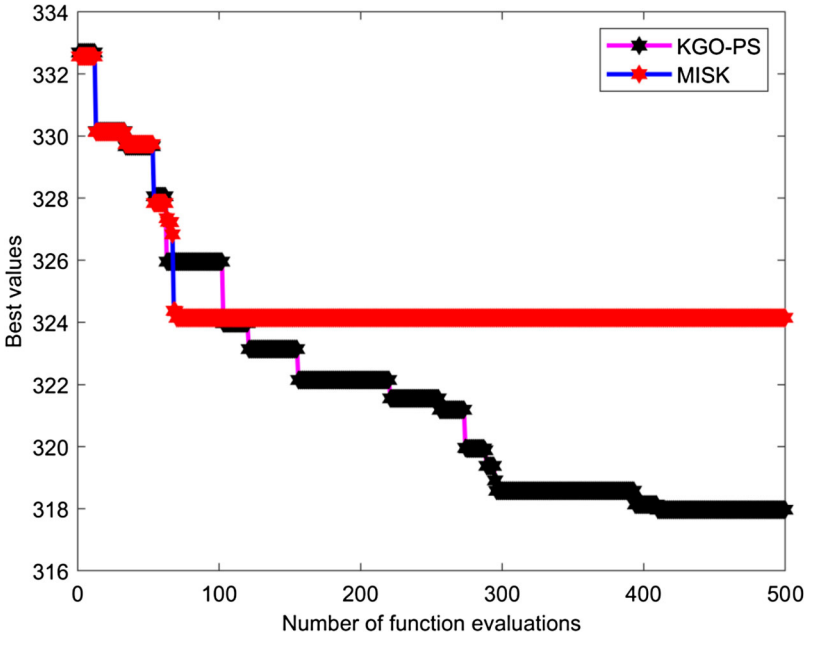

Figure 11. Iterative results based on NFE (MISK and KGO-PS).

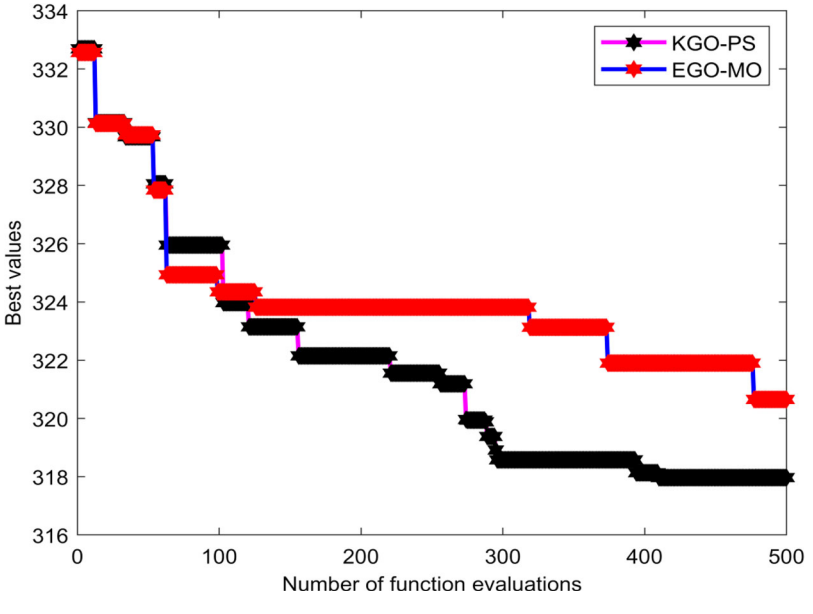

Figure 12. Iterative results based on NFE (EGO-MO and KGO-PS).

In Figures 11 and 12, the MISK obtains its best values in approximately 70 NFE. Unfortunately, the MISK will become trapped in a local valley from 70 NFE to 500 NFE. This is because the MISK will select new sampling points that have higher weight on the local exploitation and less weight on the global exploration and lacks a strategy that helps it jump out of the local valley. This condition also occurred in EGO-MO. Compared with it, the KGO-PS has a stronger ability to jump out of the local valley. It will not last long at a value, which means that the KGO-PS can make a better balance between global

Table 3. The optimization results of the simulation experiments.

Algorithm	Optimal solution	Rejection rate	NFE	Running time
Initialization without optimization	366.5	35.73%	–	–
PSO	330.4	31.69%	1000	32.2 h
EGO	324.7	26.09%	500	16.7 h
KGO-PS	317.6	24.66%	500	16.7 h
MISK	324.1	29.08%	500	16.7 h
EGO-MO	320.1	28.78%	500	16.7 h

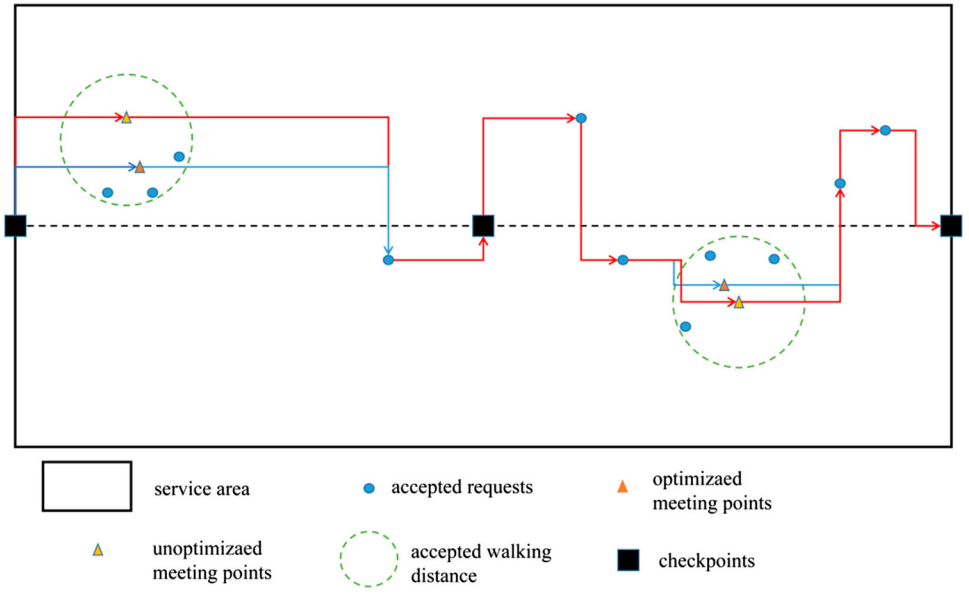

Figure 13. The influence of meeting point locations.

exploration and local exploitation. Therefore, the KGO-PS can efficiently solve expensive black-box problems.

In Table 3, experiencing 1000 NFE, the PSO can obtain the best value: 330.4. While experiencing 500 NFE, the KGO-PS, MISK, EGO-MO and EGO can obtain the best values: 317.6, 324.1, 320.1 and 324.7, respectively. This demonstrates that the KGO-PS can obtain better optimal solutions using the same or fewer computing resources, which proves that the KGO-PS is more suitable for solving expensive black-box problems in real life engineering applications. Compared with the initial solution, the KGO-PS can reduce the system cost by 12.8%. Moreover, it can also reduce the rejection rate of the flex-transit system to approximately 31%, which will attract more passengers. Therefore, it is necessary to optimize the meeting point locations and effectively improve the performance of the flex-route transit services under unexpectedly high-demand levels.

5.3. The influence of meeting point locations on the FRT-MP system performance

The flex-route transit with meeting points (FRT-MP), which was proposed by Zheng, Li, et al. (2019), is an improved mode of the traditional flex-route transit. The meeting point location is an important factor that influences the FRT-MP performance. In this section, the influence is displayed in detail (see Figure 13):

The system performance metric is composed of five parts (the cost of vehicle running, passengers' riding time, walking time, waiting time and idle time). Then, the meeting point location influencing the five parts will be demonstrated as follows:

The cost of vehicle running and passengers' riding time is mainly dependent on the time of vehicle running. In Figure 13, it can be seen that the optimized meeting points (the orange triangle) can reduce the vehicle detour effectively. Hence, the vehicle running distance is shorter. Without considering the road resistance, the vehicle running time of optimized meeting points is less than that of unoptimized meeting points (the yellow triangle). For the walking time, the optimized meeting point can be located at a suitable location, which can reduce the passengers' walking time. For the waiting time, the optimized meeting points (the orange triangle) can effectively reduce the vehicle detour. In real life, it can improve the on-time performance of vehicles and reduce passengers' walking time. For the idle time (i.e. the extra waiting time if the vehicle arrives at checkpoints before the timetable), although the optimized meeting points will increase the idle time slightly (i.e. the vehicle running time is saved, and the vehicle can arrive at the checkpoints in advance), the increase in idle time cost is far less than the reduction in other costs (vehicle running, passengers' riding time, walking time and waiting time).

In summary, suitable meeting point locations can considerably enhance the performance of the FRT-MP system, which must be optimized.

6. Conclusion

As an on-demand transportation service, flex-route transit services are promising for promoting sustainable societal development. In this work, the optimal locations of meeting points are studied to improve the performance of flex-route transit services under unexpectedly high-demand levels. By using the simulation model to reproduce the complex operating process of the flex-route transit services, the meeting point location selection is modelled as a simulation-based optimization (SO) problem. Then, a Kriging-based global optimization algorithm using a Pareto-based multipoint sampling strategy (KGO-PS) is proposed to efficiently solve the SO problem. Finally, numerical experiments and simulation experiments based on real life Line 646 have proven that the KGO-PS is more effective, reliable and brief than other well-known surrogate-based global optimization algorithms. The main contributions of this paper are summarized as follows:

(1) The key parameters of the meeting points strategy (i.e. the optimal locations of meeting points) is studied, in this way, the performance of flex-route transit services under unexpectedly high-demand levels can be improved.
(2) Considering the undeterministic passengers' travel demand, the meeting point location problem is modelled as a simulation-based optimization model based on Monte Carlo Simulation. In this way, more realistic solutions can be obtained.
(3) To address the disadvantages of *P*-EI functions, the KGO-PS algorithm is designed. It provides a novel mechanism that realizes the balance between global exploration and local exploitation. Moreover, compared with other methods, it is more effective and reliable.

However, the current work still has some limitations: (1) Solving high-dimensional expensive black-box problems is an acknowledged challenge to surrogate-based optimization algorithms. In this work, this problem also constrained the number of meeting points. Future work will improve the algorithm's performance under higher-dimension ($> 10–30$) problems. (2) The proposed algorithm is focused on solving expensive black-box problems with simple constraints or without constraints. In the future, it will be extended to solve expensive black-box problems with complex constraints.

Disclosure statement

No potential conflict of interest was reported by the author(s).

Funding

This research was funded in part by the National Natural Science Foundation of China (No. 52172310), Humanities and Social Sciences Foundation of the Ministry of Education (No. 21YJCZH147), Innovation-Driven Project of Central South University (No. 2020CX041).

References

Aïvodji, U. M., S. Gambs, M. J. Huguet, and M. O. Killijian. 2016. "Meeting Points in Ridesharing: A Privacy-Preserving Approach." *Transportation Research Part C: Emerging Technologies* 72: 239–253. doi:10.1016/j.trc.2016.09.017.

Becker, J., R. Teal, and R. Mossige. 2013. "Metropolitan Transit Agency's Experience Operating General-Public Demand-Responsive Transit." *Transportation Research Record: Journal of the Transportation Research Board* 2352: 136–145. doi:10.3141/2352-16.

Chávez, H., K. Castillo-Villar, L. Herrera, and A. Bustos. 2017. "Simulation-Based Multi-Objective Model for Supply Chains with Disruptions in Transportation." *Robotics and Computer-Integrated Manufacturing* 43: 39–49. doi:10.1016/j.rcim.2015.12.008.

Chen, P. W., and Y. M. Nie. 2017a. "Analysis of an Idealized System of Demand Adaptive Paired-Line Hybrid Transit." *Transportation Research Part B: Methodological* 102: 38–54. doi:10.1016/j.trb.2017.05.004.

Chen, P. W., and Y. M. Nie. 2017b. "Connecting e-Hailing to Mass Transit Platform: Analysis of Relative Spatial Position." *Transportation Research Part C: Emerging Technologies* 77: 444–461. doi:10.1016/j.trc.2017.02.013.

Chen, X., L. Zhang, X. He, C. Xiong, and Z. Zhu. 2018. "Simulation-Based Pricing Optimization for Improving Network-Wide Travel Time Reliability." *Transportmetrica A: Transport Science* 14 (1-2): 155–176. doi:10.1080/23249935.2017.1379038.

Chung, I., D. Park, and D. Choi. 2018. "Surrogate-Based Global Optimization Using an Adaptive Switching Infill Sampling Criterion for Expensive Black-Box Functions." *Structural and Multidisciplinary Optimization* 57: 1443–1459. doi:10.1007/s00158-018-1942-2.

Czioska, P., D. C. Mattfeld, and M. Sester. 2017. "GIS-Based Identification and Assessment of Suitable Meeting Point Locations for Ride-Sharing." *Transportation Research Procedia* 22: 314–324. doi:10.1016/j.trpro.2017.03.038.

Dong, H., B. Song, Z. Dong, and P. Wang. 2016. "Multi-Start Space Reduction (MSSR) Surrogate-Based Global Optimization Method." *Structural and Multidisciplinary Optimization* 54: 907–926. doi:10.1007/s00158-016-1450-1.

Dong, H., B. Song, Z. Dong, and P. Wang. 2018a. "SCGOSR: Surrogate-Based Constrained Global Optimization Using Space Reduction." *Applied Soft Computing* 65: 462–477. doi:10.1016/j.asoc.2018.01.041.

Dong, H., B. Song, P. Wang, and Z. Dong. 2018b. "Hybrid Surrogate-Based Optimization Using Space Reduction (HSOSR) for Expensive Black-Box Functions." *Applied Soft Computing* 64: 641–655. doi:10.1016/j.asoc.2017.12.046.

Dong, H., S. Sun, B. Song, and P. Wang. 2019. "Multi-Surrogate-Based Global Optimization Using a Score-Based Infill Criterion." *Structural and Multidisciplinary Optimization* 59: 485–506. doi:10.1007/s00158-018-2079-z.

Farwell, R., and E. Marx. 1996. "Planning, Implementation, and Evaluation of Omniride Demand-Driven Transit Operations: Feeder and Flex-Route Services." *Transportation Research Record: Journal of the Transportation Research Board* 1557: 1–9. doi:10.1177/0361198196155700101.

Feng, Z., Q. B. Zhang, Q. F. Zhang, Q. Tang, T. Yang, and Y. Ma. 2015. "A Multiobjective Optimization Based Framework to Balance the Global Exploration and Local Exploitation in Expensive Optimization." *Journal of Global Optimization* 61: 677–694. doi:10.1007/s10898-014-0210-2.

Fittante, S. R., and A. Lubin. 2015. "Adapting the Swedish Service Route Model to Suburban Transit in the United States." *Transportation Research Record* 2536: 52–59. doi:10.3141/2536-07.

Gkiotsalitis, K., and O. Cats. 2019. "Multi-Constrained Bus Holding Control in Time Windows with Branch and Bound and Alternating Minimization." *Transportmetrica B: Transport Dynamics* 7 (1): 1258–1285. doi:10.1080/21680566.2019.1606743.

Gu, J. 2021. "An Efficient Multiple Meta-Model-Based Global Optimization Method for Computationally Intensive Problems." *Advances in Engineering Software* 152: 102958. doi:10.1016/j.advengsoft.2020.102958.

Gutmann, H. M. 2001. "A Radial Basis Function Method for Global Optimization." *Journal of Global Optimization* 19 (3): 201–227. doi:10.1023/A:1011255519438.

Haftka, R. T., D. Villanueva, and A. Chaudhuri. 2016. "Parallel Surrogate-Assisted Global Optimization with Expensive Functions – A Survey." *Structural and Multidisciplinary Optimization* 54 (1): 3–13. doi:10.1007/s00158-016-1432-3.

Hao, S., R. Song, and S. He. 2022. "Timetabling for a Congested Urban Rail Transit Network Based on Mixed Logic Dynamic Model." *Transportmetrica B: Transport Dynamics* 10 (1): 139–158. doi:10.1080/21680566.2021.1965925.

Huang, Y., D. Sun, and S. Zhang. 2022. "Three-Dimensional Macroscopic Fundamental Diagram for Car and Bicycle Heterogeneous Traffic." *Transportmetrica B: Transport Dynamics* 10 (1): 312–339. doi:10.1080/21680566.2021.1994050.

Jones, D. R. 2001. "A Taxonomy of Global Optimization Methods Based on Response Surfaces." *Journal of Global Optimization* 21: 345–383. doi:10.1023/A:1012771025575.

Jones, D. R., M. Schonlau, and W. J. Welch. 1998. "Efficient Global Optimization of Expensive Black-Box Functions." *Journal of Global Optimization* 13 (4): 455–492. doi:10.1023/A:1008306431147.

Kim, S., S. Rasouli, H. Timmermans, and D. Yang. 2022. "A Scenario-Based Stochastic Programming Approach for the Public Charging Station Location Problem." *Transportmetrica B: Transport Dynamics* 10 (1): 340–367. doi:10.1080/21680566.2021.1997672.

Koffman, D. 2004. *Operational Experiences with Flexible Transit Services: A Synthesis of Transit Practice*. TCRP Synthesis 53. Washington, DC: Transportation Research Board.

Koullias, S., and D. N. Mavris. 2014. "Methodology for Global Optimization of Computationally Expensive Design Problems." *Journal of Mechanical Design* 136 (8): 081007. doi:10.1115/1.4027493.

Li, M., Y. Bing, and Y. Yang. 2022. "An Efficient Global Optimization Method with Multi-Point Infill Sampling Based on Kriging." *Engineering Optimization* 54: 1801–1818. doi:10.1080/0305215X.2021.1960985.

Liu, R., Y. Tao, Q. Hu, and X. Xie. 2017. "Simulation-Based Optimisation Approach for the Stochastic Two-Echelon Logistics Problem." *International Journal of Production Research* 55 (1): 187–201. doi:10.1080/00207543.2016.1201221.

Liu, M., J. Zhang, S. Hoogendoorn, and M. Wang. 2022. "An Optimal Control Approach of Integrating Traffic Signals and Cooperative Vehicle Trajectories at Intersections." *Transportmetrica B: Transport Dynamics* 10 (1): 971–987. doi:10.1080/21680566.2021.1991505.

Long, T., D. Wu, X. Guo, G. G. Wang, and L. Liu. 2015. "Efficient Adaptive Response Surface Method Using Intelligent Space Exploration Strategy." *Structural and Multidisciplinary Optimization* 51 (6): 1335–1362. doi:10.1007/s00158-014-1219-3.

Potts, J. F., M. A. Marshall, E. C. Crockett, and J. Washington. 2010. *A Guide for Planning and Operating Flexible Public Transportation Services*. TCRP Report 140. Washington, DC: Transportation Research Board.

Qian, X., W. Zhang, S. V. Ukkusuri, and C. Yang. 2017. "Optimal Assignment and Incentive Design in the Taxi Group Ride Problem." *Transportation Research Part B: Methodological* 103: 208–226. doi:10.1016/j.trb.2017.03.001.

Qiu, F., W. Li, and A. Haghani. 2015. "A Methodology for Choosing between Fixed-Route and Flex-Route Policies for Transit Services." *Journal of Advanced Transportation* 49 (3): 496–509. doi:10.1002/atr.1289.

Qiu, F., W. Li, and J. Zhang. 2014. "A Dynamic Station Strategy to Improve the Performance of Flex-Route Transit Services." *Transportation Research Part C: Emerging Technologies* 48: 229–240. doi:10.1016/j.trc.2014.09.003.

Quadrifoglio, L., M. M. Dessouky, and F. Ordóñez. 2008. "Mobility Allowance Shuttle Transit (MAST) Services: MIP Formulation and Strengthening with Logic Constraints." *European Journal of Operational Research* 185 (2): 481–494. doi:10.1016/j.ejor.2006.12.030.

Quadrifoglio, L., M. M. Dessouky, and K. Palmer. 2007. "An Insertion Heuristic for Scheduling Mobility Allowance Shuttle Transit (MAST) Services." *Journal of Scheduling* 10 (1): 25–40. doi:10.1007/s10951-006-0324-6.

Regis, R. G., and C. A. Shoemaker. 2007. "A Stochastic Radial Basis Function Method for the Global Optimization of Expensive Functions." *INFORMS Journal on Computing* 19 (4): 497–509. doi:10.1287/ijoc.1060.0182.

Sacks, J., W. J. Welch, T. J. Mitchell, and H. P. Wynn. 1989. "Design and Analysis of Computer Experiments." *Statistical Science* 4 (4): 409–423. doi:10.1214/ss/1177012413.

Schmaranzer, D., R. Braune, and K. Doerner. 2020. "Population-Based Simulation Optimization for Urban Mass Rapid Transit Networks." *Flexible Services and Manufacturing Journal* 32 (4): 767–805. doi:10.1007/s10696-019-09352-9.

Shi, H., S. Xie, and X. Wang. 2013. "A Warpage Optimization Method for Injection Molding Using Artificial Neural Network with Parametric Sampling Evaluation Strategy." *The International Journal of Advanced Manufacturing Technology* 65: 343–353. doi:10.1007/s00170-012-4173-5.

Sobester, A., S. Leary, and A. Keane. 2005. "On the Design of Optimization Strategies Based on Global Response Surface Approximation Models." *Journal of Global Optimization* 33: 31–59. doi:10.1007/s10898-004-6733-1.

Velaga, N. R., J. D. Nelson, S. D. Wright, and J. H. Farrington. 2012. "The Potential Role of Flexible Transport Services in Enhancing Rural Public Transport Provision." *Journal of Public Transportation* 15 (1): 111–131. doi:10.5038/2375-0901.15.1.7.

Viana, F., R. Haftka, and L. Watson. 2013. "Efficient Global Optimization Algorithm Assisted by Multiple Surrogate Techniques." *Journal of Global Optimization* 56: 669–689. doi:10.1007/s10898-012-9892-5.

Winston, W. L., M. Venkataramanan, and J. B. Goldberg. 2003. *Introduction to Mathematical Programming*. Pacific Grove, CA: Thomson/Brooks/Cole.

Wu, Y., L. Teng, R. Shi, and G. Wang. 2021. "Mode-Pursuing Sampling Method Using Discriminative Coordinate Perturbation for High-Dimensional Expensive Black-Box Optimization." *Journal of Mechanical Design* 143 (4): 041703. doi:10.1115/1.4047909.

Xing, J., Y. Luo, and Z. Gao. 2020. "A Global Optimization Strategy Based on the Kriging Surrogate Model and Parallel Computing." *Structural and Multidisciplinary Optimization* 62 (1): 405–417. doi:10.1007/s00158-020-02495-6.

Xiong, C., Z. Zhu, X. Chen, and L. Zhang. 2018. "Optimal Travel Information Provision Strategies: An Agent-Based Approach under Uncertainty." *Transportmetrica B: Transport Dynamics* 6 (2): 129–150. doi:10.1080/21680566.2017.1336126.

Zhan, D., J. Qian, and Y. Cheng. 2017a. "Balancing Global and Local Search in Parallel Efficient Global Optimization Algorithms." *Journal of Global Optimization* 67: 873–892. doi:10.1007/s10898-016-0449-x.

Zhan, D., J. Qian, and Y. Cheng. 2017b. "Pseudo Expected Improvement Criterion for Parallel EGO Algorithm." *Journal of Global Optimization* 68: 641–662. doi:10.1007/s10898-016-0484-7.

Zhang, Q., and H. Li. 2007. "MOEA/D: A Multiobjective Evolutionary Algorithm Based on Decomposition." *IEEE Transactions on Evolutionary Computation* 11 (6): 712–731. doi:10.1109/TEVC.2007.892759.

Zheng, Y., W. Li, and F. Qiu. 2018. "A Slack Arrival Strategy to Promote Flex-Route Transit Services." *Transportation Research Part C: Emerging Technologies* 92: 442–455. doi:10.1016/j.trc.2018.05.015.
Zheng, Y., W. Li, F. Qiu, and H. Wei. 2019. "The Benefits of Introducing Meeting Points into Flex-Route Transit Services." *Transportation Research Part C: Emerging Technologies* 106: 98–112. doi:10.1016/j.trc.2019.07.012.
Zheng, L., X. Xue, C. Xu, and B. Ran. 2019. "A Stochastic Simulation-Based Optimization Method for Equitable and Efficient Network-Wide Signal Timing under Uncertainties." *Transportation Research Part B: Methodological* 122: 287–308. doi:10.1016/j.trb.2019.03.001.

Appendices

Appendix A. The derivation of the properties of P_1 and P_2

As Formulas (18) and (19) shown:

$$P_1 = [(y_{\min} - y(x))]\Phi\left(\frac{y_{\min} - y(x)}{P * s(x)}\right) \tag{35}$$

$$P_2 = P * s(x)\varphi\left(\frac{y_{\min} - y(x)}{P * s(x)}\right) \tag{36}$$

Learning from Zhan, Qian, and Cheng (2017b), the search property of the second term of the traditional EI function is mainly dependent on $s(x)$, and the influence of $y(x)$ can generally be overlooked. The second term of EI can be regarded as a special condition of P_2 when $P = 1$. Observing the formulation of P_2, the parameter P will further increase the influence of $s(x)$ compared with the second term of the traditional EI function. Therefore, the influence of $y(x)$ is approximately overlooked in this article. Therefore, the partial derivative of P_2 with respect to $s(x)$ is given as:

$$\frac{\partial(P_2)}{\partial(s(x))} = P * \left[\varphi\left(\frac{y_{\min} - y(x)}{P * s(x)}\right) + \left(\left(\frac{y_{\min} - y(x)}{P * s(x)}\right)^2\right) * \varphi\left(\frac{y_{\min} - y(x)}{P * s(x)}\right)\right] \tag{37}$$

Due to $0 < \Phi < 1, 0 < \varphi$ and $s(x) > 0$, it is obvious that:

$$\frac{\partial(P_2)}{\partial(s(x))} > 0 \tag{38}$$

This means that P_2 is positively correlated with $s(x)$. Therefore, maximizing P_2 requires $s(x)$ to be as large as possible; in other words, it searches points with high uncertainty. P_2 represents global exploration.

Then, the partial derivatives of P_1 with respect to $y(x)$ and $s(x)$ are given as:

$$\frac{\partial(P_1)}{\partial(y(x))} = -\Phi\left(\frac{y_{\min} - y(x)}{P * s(x)}\right) - \frac{y_{\min} - y(x)}{P * s(x)} * \varphi\left(\frac{y_{\min} - y(x)}{P * s(x)}\right) \tag{39}$$

$$\frac{\partial(P_1)}{\partial(s(x))} = -\frac{(y_{\min} - y(x))^2}{P * s(x) * s(x)} * \varphi\left(\frac{y_{\min} - y(x)}{P * s(x)}\right) \tag{40}$$

Due to $0 < \Phi < 1, 0 < \varphi$, and $s(x) > 0$, it is obvious that:

$$\frac{\partial(P_1)}{\partial(s(x))} < 0 \tag{41}$$

This means that P_1 is negatively correlated with $s(x)$. Since Kriging is a type of interpolation model, at least one point whose prediction value $y(x)$ is less than or equal to $y_{\min}$ exists. When maximizing P_1, we only need to consider the following condition: $y(x) \leq y_{\min}$ because if $y(x) > y_{\min}, P_1 < 0$; if $y(x) \leq y_{\min}, P_1 \geq 0$. Under this condition:

$$\frac{\partial(P_1)}{\partial(y(x))} < 0 \tag{42}$$

Therefore, maximizing P_1 requires that $y(x)$ and $s(x)$ be as small as possible. In other words, the point maximizing P_1 has small prediction values and low uncertainty, and P_1 places emphasis on exploiting the predictor and no emphasis on exploring points that are uncertain. Maximizing P_1 represents local exploitation.

Appendix B. An example to illustrate the disadvantage of the *P*-EI function

Consider a function:

$$y = (6x - 2)^2 \sin(12x - 4), \quad 0 < x < 1 \tag{43}$$

The Kriging model is constructed by six points (0, 0.1, 0.2, 0.3, 0.4, 1), and the new sampling point is obtained by maximizing the *P*-EI function, P_1, P_2. For illustrative purposes only, here, the value of parameter P is set to 1.

Figure A1 shows the Kriging prediction function (the red line) constructed by the six points and the real function (the purple line). Figure A2 gives the *P*-EI, P_1, P_2 function curve (the red, purple and blue lines) and points obtained by maximizing the *P*-EI, P_1, and P_2 functions. It is obvious that in this process of obtaining new sampling points, the point obtained by maximizing the *P*-EI function is the same as the point obtained by maximizing the P_1 function. Therefore, unfortunately, in this example, it can be concluded that the *P*-EI function is only for local exploitation while ignoring global exploration.

Appendix C. Multiobjective evolutionary algorithm based on decomposition (MOEA/D)

MOEA/D is one of the most popular algorithms for solving biobjective optimization problems (Zhang and Li 2007). The MOEA/D basis is the decomposition strategy. The decomposition into multiple scalar optimization subproblems refers to: instead of processing as a whole, decomposing one into a single-objective optimization problem. The decomposition is achieved through the polymerization method. Due to its good performance in nonlinear problems, the Chebyshev method is the most commonly used method, which can be seen as follows:

$$\min : g^{tch}(x|\lambda, z) = \max\{\lambda_i|f_i(x) - z_i|\} \tag{44}$$

$$s.t. \quad x \in D \tag{45}$$

where *tch* represents the Chebyshev decomposition method and *z* is the reference point, $z = (z_1, z_2 \ldots ., z_m)^T$. For each $i = 1, 2 \ldots , m. z_i = \min f_i(x)$, *m* is the target number of the multiobjective optimization problem. f_i is the *i*-th objective function of the multiobjective problem. The setting of the reference point can make the population distribution more uniform and improve the algorithm effect.

The pseudocode of MOEA/D is summarized in Algorithm 3:

Appendix D. The benchmark function used in the numerical experiments

1. F1 function

$$y = {x_1}^2 + {x_2}^2 - \cos(18x_1) - \cos(18x_2) \tag{46}$$

2. Ackley (AK) function

$$y = 20 + \exp(-20 * \exp(-0.2 * (0.5{x_1}^2 + 0.5{x_2}^2)^{0.5}) - \exp(0.5\cos(2\pi x_1 + 2\pi x_2)) \tag{47}$$

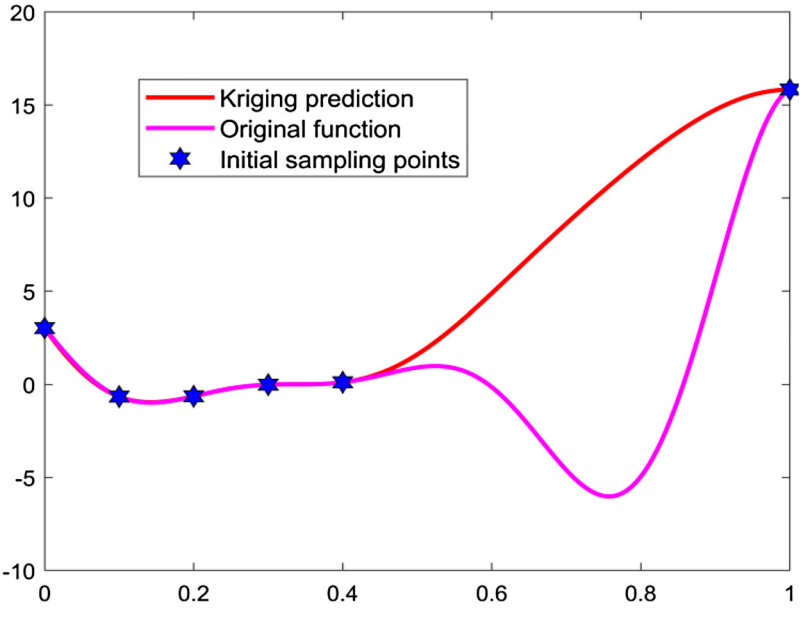

Figure A1. Kriging and original function of the example function.

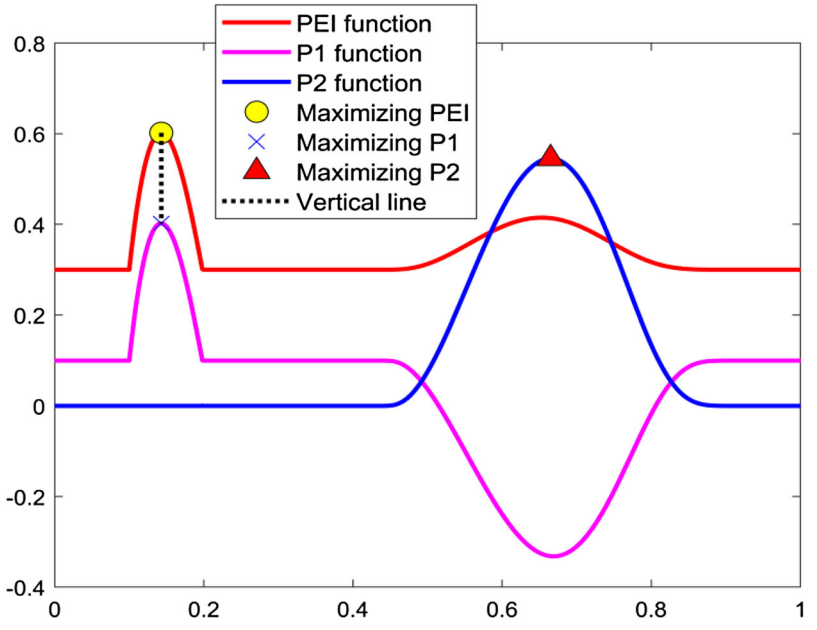

Figure A2. Sampling points obtained by maximizing P-EI, P_1 and P_2 (i.e. To facilitate identification, each function curve has been shifted up or down).

Algorithm 3. MOEA/D

Input: a multiobjective optimization problem: min: $f_1(x), f_2(x) \dots, f_m(x)$
A stop condition: the maximum number of iterations Gen.
The size of population: N
A set of weight vectors: $\lambda = (\lambda_j^1, \dots, \lambda_j^i)$: $i = 1, 2, \dots, N; j = 1, 2, \dots, m$.
Number of neighbours: T
Output: Approximate Pareto Frontier: EP.
1. **Initialization**
2. suppose $EP = \emptyset$ (The $\emptyset$ represents an empty set).

3. Hartman6 (H6) function

$$y = -\sum_{i=1}^{4} \alpha_i \exp\left[-\sum_{j=1}^{6} B_{ij}(x_j - Q_{ij})^2\right] \tag{48}$$

$$\alpha = [1, 1.2, 3, 3.2]^T \tag{49}$$

$$B = \begin{bmatrix} 10 & 3 & 17 & 3.5 & 1.7 & 8 \\ 0.05 & 10 & 17 & 0.1 & 8 & 14 \\ 3 & 3.5 & 1.7 & 10 & 17 & 8 \\ 17 & 8 & 0.05 & 10 & 0.1 & 14 \end{bmatrix} \tag{50}$$

$$Q = 10^{-4} \begin{bmatrix} 1312 & 1696 & 5569 & 124 & 8283 & 5886 \\ 2329 & 4135 & 8307 & 3736 & 1004 & 9991 \\ 2348 & 1451 & 3522 & 2883 & 3047 & 6650 \\ 4047 & 8828 & 8732 & 5743 & 1091 & 381 \end{bmatrix} \tag{51}$$

4. Trid Function (TF)

$$y = \sum_{i=1}^{6} (x_i - 1)^2 - \sum_{i=2}^{6} x_i x_{i-1} \tag{52}$$

3. Calculate the distance between each weight vector and the ownership vector, take the nearest T weight vectors of each weight vector, and store their index in B. For each $i = 1, 2, \ldots, N$, $B(i) = \{i_1, i_2, \ldots, i_T\}$.
4. Randomly or by other methods to generate initial population: $x^1, x^2, \ldots, x^N$.
5. For each $i = 1, 2, \ldots, N$, set $FV_i = F(x^i)$.
6. Initialize reference point z.
7. ***while*** the stop condition is not met
8. ***for*** $i = 1{:}N$
9. Generate offspring: randomly select two indices k and l from $B(i)$, and use analog binary crossover operator to generate offspring individuals $x*$ from x^k and x^l.
10. Adjustment: if necessary (out of bounds, etc.), then adjust $x*$.
11. Calculate the objective function value $F(x*)$.
12. ***for*** $j = 1{:}m$
13. ***if*** $f_j(x*) < z_j$
14. $z_j = f_j(x*)$
15. ***else***
16. $z_j = z_j$
17. ***end***
18. ***end***
19. ***for*** $j = 1{:}\text{sum}(B(i))$
20. ***if*** $g^{\text{tch}}(x* \mid \lambda^j, z) \leq g^{tch}(x^j \mid \lambda^j, z)$
21. $x^j = x*, FV_j = F(x*)$
22. ***else***
23. $x^j = x^j, FV_j = FV_j$
24. ***end***
25. ***end***
26. Update EP: First delete all target vectors dominated by $F(x*)$ in EP, then add the $F(x*)$ to EP.
27. ***end*** % corresponds to the *for* in Line 8
28. ***end*** % corresponds to the *while* in Line 7
29. **END**

5. Paviani function (PAF)

$$y = \sum_{i=1}^{10} [\ln^2(x_i - 2) + \ln^2(10 - x_i)] - \left(\prod_{i=1}^{10} x_i\right)^{0.2} \tag{53}$$

6. F16 function

$$y = \sum_{i=1}^{16}\sum_{j=1}^{16} a_{ij}({x_i}^2 + x_i + 1)({x_j}^2 + x_j + 1) \tag{54}$$

$$(\text{row}: 1-8)a_{ij} = \begin{bmatrix} 1 & 0 & 0 & 1 & 0 & 0 & 1 & 1 & 0 & 0 & 0 & 0 & 0 & 0 & 0 & 1 \\ 0 & 1 & 1 & 0 & 0 & 0 & 1 & 0 & 0 & 1 & 0 & 0 & 0 & 0 & 0 & 0 \\ 0 & 0 & 1 & 0 & 0 & 0 & 1 & 0 & 1 & 1 & 0 & 0 & 0 & 1 & 0 & 0 \\ 0 & 0 & 0 & 1 & 0 & 0 & 1 & 0 & 0 & 0 & 1 & 0 & 0 & 0 & 1 & 0 \\ 0 & 0 & 0 & 0 & 1 & 1 & 0 & 0 & 0 & 1 & 0 & 1 & 0 & 0 & 0 & 1 \\ 0 & 0 & 0 & 0 & 0 & 1 & 0 & 1 & 0 & 0 & 0 & 0 & 0 & 0 & 1 & 0 \\ 0 & 0 & 0 & 0 & 0 & 0 & 1 & 0 & 0 & 0 & 1 & 0 & 1 & 0 & 0 & 0 \\ 0 & 0 & 0 & 0 & 0 & 0 & 0 & 1 & 0 & 1 & 0 & 0 & 0 & 0 & 1 & 0 \end{bmatrix} \tag{55}$$

$$(\text{row}: 9-16)a_{ij} = \begin{bmatrix} 0 & 0 & 0 & 0 & 0 & 0 & 0 & 0 & 1 & 0 & 0 & 1 & 0 & 0 & 0 & 1 \\ 0 & 0 & 0 & 0 & 0 & 0 & 0 & 0 & 0 & 1 & 0 & 0 & 0 & 1 & 0 & 0 \\ 0 & 0 & 0 & 0 & 0 & 0 & 0 & 0 & 0 & 0 & 1 & 0 & 1 & 0 & 0 & 0 \\ 0 & 0 & 0 & 0 & 0 & 0 & 0 & 0 & 0 & 0 & 0 & 1 & 0 & 1 & 0 & 0 \\ 0 & 0 & 0 & 0 & 0 & 0 & 0 & 0 & 0 & 0 & 0 & 0 & 1 & 1 & 0 & 0 \\ 0 & 0 & 0 & 0 & 0 & 0 & 0 & 0 & 0 & 0 & 0 & 0 & 0 & 1 & 0 & 0 \\ 0 & 0 & 0 & 0 & 0 & 0 & 0 & 0 & 0 & 0 & 0 & 0 & 0 & 0 & 1 & 0 \\ 0 & 0 & 0 & 0 & 0 & 0 & 0 & 0 & 0 & 0 & 0 & 0 & 0 & 0 & 0 & 1 \end{bmatrix} \tag{56}$$

7. Sum Squares function (SF)

$$y = \sum_{i=1}^{12/20} i * {x_i}^2 \tag{57}$$

8. SS function

$$y = \sum_{i=1}^{10} i * {x_i}^2 \tag{58}$$

9. ED function

$$y = \sum_{i=1}^{10/12} \sum_{j=1}^{i} {x_j}^2 \tag{60}$$

Appendix E

Table E1. Comparison of EGO and other algorithms.

Function	Standard		KGO-PS	EGO	EGO-MO	MISK
F1	OS	Mean	**−2**	−1.9991	−1.9935	−1.7336
		Variance	**0**	7.0278e-7	1.3984e-4	0.0346
AK	OS	Mean	**0.0366**	0.1137	0.0563	0.5245
		Variance	**0.0013**	0.0080	0.0017	1.043
ED10	OS	Mean	**0.00625**	1.9840	0.0284	0.1241
		Variance	**2.0334e-6**	1.6460	0.0048	0.0289
ED12	OS	Mean	**0.0027**	1.8240	0.0056	0.0079
		Variance	**1.0334e-6**	0.1678	2.7965e-5	1.7985e-5
SS	OS	Mean	**0.0012**	3.7192	0.0562	0.0246
		Variance	**2.853e-5**	0.7767	0.0365	0.0028
SF12	OS	Mean	**0.0035**	0.3518	0.0145	0.0079
		Variance	**3.4528e-7**	0.0075	0.0092	5.4892e-6
H6	OS	Mean	**−3.3095**	−3.0263	−3.2842	−3.3005
		Variance	**0.0029**	0.0185	0.0046	0.0041
TF	OS	Mean	−49.56	−40.91	−46.9378	**−49.9921**
		Variance	0.1606	14.9129	3.3716	**3.6144e-5**
PAF	OS	Mean	**−45.5**	−44.0781	−44.549	−45.3212
		Variance	0.0407	0.3209	0.2363	**0.0194**
F16	OS	Mean	**25.875**	36.2879	**25.875**	**25.875**
		Variance	**0**	2.2745	**0**	**0**
SF20 (SSF)	OS	Mean	0.5233	11.9664	**0.4063**	8.1408
		Variance	0.0455	1.2181	**0.0105**	15.7272